

# A beginner's guide to low-coverage whole genome sequencing for population genomics

Runyang Nicolas Lou<sup>1\*</sup>, Arne Jacobs<sup>1,2</sup>, Aryn Wilder<sup>3</sup>, Nina O. Therkildsen<sup>1\*</sup>

<sup>1</sup>Department of Natural Resources and the Environment, Cornell University, Ithaca, NY 14853, USA

<sup>2</sup>Current address: Institute of Biodiversity, Animal Health and Comparative Medicine, University of Glasgow, Glasgow, G12 8QQ, UK

<sup>3</sup>San Diego Zoo Wildlife Alliance, Escondido, CA 92027, USA

\*Corresponding authors: RNL ([rl683@cornell.edu](mailto:rl683@cornell.edu)), NOT ([nt246@cornell.edu](mailto:nt246@cornell.edu))

## Abstract

Low-coverage whole genome sequencing (lcWGS) has emerged as a powerful and cost-effective approach for population genomic studies in both model and non-model species. However, with read depths too low to confidently call individual genotypes, lcWGS requires specialized analysis tools that explicitly account for genotype uncertainty. A growing number of such tools have become available, but it can be difficult to get an overview of what types of analyses can be performed reliably with lcWGS data, and how the distribution of sequencing effort between the number of samples analyzed and per-sample sequencing depths affects inference accuracy. In this introductory guide to lcWGS, we first illustrate how the per-sample cost for lcWGS is now comparable to RAD-seq and Pool-seq in many systems. We then provide an overview of software packages that explicitly account for genotype uncertainty in different types of population genomic inference. Next, we use both simulated and empirical data to assess the accuracy of allele frequency and genetic diversity estimation, detection of population structure, and selection scans under different sequencing strategies. Our results show that spreading a given amount of sequencing effort across more samples with lower depth per sample consistently improves the accuracy of most types of inference, with a few notable exceptions. Finally, we assess the potential for using imputation to bolster inference from lcWGS data in non-model species, and discuss current limitations and future perspectives for lcWGS-based population genomics research. With this overview, we hope to make lcWGS more approachable and stimulate its broader adoption.

**Keywords:** genotype likelihoods, bioinformatics, allele frequencies, population structure, selection scan, genotype imputation

## 38 1. Introduction

39

40 Despite massive reductions in the cost of DNA sequencing over the past decades, researchers  
41 remain faced with decisions about how to distribute sequencing effort along three dimensions:  
42 1) how much of the genome to sequence (breadth of coverage), 2) how deeply to sequence each  
43 sample (depth of coverage), and 3) the total number of samples to sequence. Until recently,  
44 reduced-representation sequencing (e.g. RAD-seq), through which a small random portion of  
45 the genome can be sequenced deeply in many individuals to allow for simultaneous variant  
46 discovery and high-confidence genotyping, has been the most popular approach for population  
47 genomics of non-model organisms (Andrews, Good, Miller, Luikart, & Hohenlohe, 2016; Davey  
48 et al., 2011; McKinney, Larson, Seeb, & Seeb, 2017). While this approach undoubtedly has led  
49 to a breakthrough in our ability to examine genome-wide patterns of variation, an important  
50 limitation is that large stretches of the genome between markers remain unsampled (Figure 1A).  
51 Accordingly, RAD-seq data may miss signatures of selection and adaptive divergence that are  
52 highly localized in the genome (Lowry et al., 2017; Tiffin & Ross-Ibarra, 2014).

53

54 In a growing number of cases, whole genome sequencing has identified striking peaks of  
55 differentiation or strong associations with phenotypes that went completely undetected with  
56 RAD-seq data (see e.g. Aguillon, Walsh, & Lovette, 2020 vs. Aguillon, Campagna, Harrison, &  
57 Lovette, 2018; Campagna, Gronau, Silveira, Siepel, & Lovette, 2015 vs. Campagna et al., 2017;  
58 Clucas, Lou, Therkildsen, & Kovach, 2019 vs. Clucas et al., 2019; and Szarmach, Brelsford,  
59 Witt, & Toews, 2021), suggesting that full genome coverage often is needed to understand  
60 mechanisms of adaptation. However, whole genome sequencing at sufficient depths to  
61 confidently call individual genotypes is still prohibitively expensive on a population scale for  
62 many projects. A popular cost-effective alternative is to sequence pools of individuals (Pool-seq;  
63 Schlötterer, Tobler, Kofler, & Nolte, 2014). When the number of individuals pooled and  
64 sequencing depth are sufficient, Pool-seq is a powerful approach for obtaining reliable estimates  
65 of population-level parameters (Futschik & Schlötterer, 2010; Zhu, Bergland, González, &  
66 Petrov, 2012). However, all information about individuals is lost, making it difficult to control for  
67 uneven contribution to the pool and precluding individual-level analyses as well as detection of  
68 cryptic substructure among sampled individuals (Anderson, Skaug, & Barshis, 2014; Fuentes-  
69 Pardo & Ruzzante, 2017).

70

71 Low-coverage whole genome sequencing (lcWGS) is emerging as a cost-effective alternative  
72 that allows population-scale screening of the entire genome while retaining individual  
73 information for - in many cases - a comparable cost to RAD-seq and Pool-seq. The underlying  
74 strategy is to maximize the information content in the sequence data by spreading it across the  
75 entire genomes of many separately barcoded individuals (Figure 1C). This way, we sacrifice  
76 depth of coverage (repeated sequencing of the same locus in the same individual), and  
77 therefore confidence in individual genotypes, in return for much greater breadth of coverage and  
78 potentially also larger sample sizes.

79

80 At low depth of coverage, individual genotypes cannot reliably be inferred (Nielsen,  
81 Korneliussen, Albrechtsen, Li, & Wang, 2012; Nielsen, Paul, Albrechtsen, & Song, 2011).

82 However, for most population-level questions, it is not the specific genotype of any particular  
83 individual that matters, but rather the overall population characteristics (e.g. allele frequencies,  
84 linkage disequilibrium (LD) patterns, etc). Similarly, for questions about genetic relationships  
85 between individuals, it is not the genotype at any particular single nucleotide polymorphism  
86 (SNP) that matters, but rather patterns of variation across SNPs genome-wide. Accordingly,  
87 probabilistic analysis frameworks that account for uncertainty about the true genotype (instead  
88 of assuming that any one genotype is correct) can integrate over the uncertainty about  
89 individual genotypes for population-level inference of variation at particular SNPs, and integrate  
90 over the uncertainty about an individual's genotype at each particular SNP to make inference  
91 about that individual's overall genetic signature (e.g. level of inbreeding, admixture proportions)  
92 (Buerkle & Gompert, 2013; Nielsen et al., 2012, 2011).

93  
94 Simulation studies have demonstrated that when sequencing data are analyzed within this type  
95 of probabilistic statistical framework that accounts for genotype uncertainty, sampling many  
96 individuals each at low read depth actually provides more accurate estimates of many  
97 population parameters than higher read depth for fewer individuals (Buerkle & Gompert, 2013;  
98 Fumagalli, 2013; Nevado, Ramos-Onsins, & Perez-Enciso, 2014). In fact, these studies have  
99 suggested that spreading sequencing depth to 1–2 reads per locus and individual (1–2x  
100 coverage or less) - and increasing sample sizes accordingly - maximizes the information gained  
101 about a population. Many recent empirical studies have demonstrated the power of this  
102 approach (examples are listed in Table S1). Some of the first applications included identification  
103 of genomic regions repeatedly associated with marine-freshwater adaptation in stickleback  
104 (Jones et al., 2012), adaptation to an Arctic lifestyle in polar bears (Liu et al., 2014), and  
105 divergence among killer whale ecotypes (Foote et al., 2016). More recently, lcWGS was used to  
106 identify genes involved in rapid adaptation to fisheries-induced size selection in experimental  
107 populations of Atlantic silversides (Therkildsen et al., 2019), map hybrid incompatibility genes in  
108 swordtail fish (Powell et al., 2020), scan for soft sweeps in response to white-nose syndrome in  
109 bats (Gignoux-Wolfsohn et al., 2021), build ultra-dense crossover maps in *Arabidopsis* (Rowan  
110 et al., 2019), and assess admixture patterns and elevated differentiation across massive linkage  
111 blocks along environmental gradients in several marine organisms (Clucas et al., 2019; Mérot et  
112 al., 2021; Wilder, Palumbi, Conover, & Therkildsen, 2020).

113  
114 Despite the clear promise, adopting a lcWGS approach can seem daunting because working  
115 with genomic data in a probabilistic framework requires both a shift in the way we think about  
116 our data and a different toolbox that incorporates genotype uncertainty in downstream analysis.  
117 In recent years, there has been a proliferation of programs that can explicitly account for  
118 genotype uncertainty in population genomic inference. But for the newcomer, it can be difficult  
119 to get an overview of what types of analyses can reliably be performed with this data type and  
120 what experimental designs will provide the most robust results for a particular system and  
121 question, e.g. how to best divide a given sequencing effort between the number of samples vs.  
122 the depth of sequencing per sample.

123  
124 The goal of this paper is to provide a practical “field guide” for researchers considering a lcWGS  
125 approach. We first illustrate that lcWGS is now a feasible option for many research projects by

126 comparing the current costs and requirements of lcWGS to alternative sequencing strategies  
127 (Section 2). Next, we introduce the basic statistical framework used to account for genotype  
128 uncertainty inherent to lcWGS data, and provide an overview of current analytical tools built  
129 under a probabilistic framework to help readers identify software that can robustly perform  
130 common types of population genomics inference with lcWGS data (Section 3). To guide  
131 experimental design, we then use both genetic simulations (Section 4) and downsampling of  
132 empirical data (Section 5) to assess the accuracy of population genomic inference under  
133 different sequencing strategies. We evaluate trade-offs between sample size and depth of  
134 coverage, compare the power of lcWGS to RAD-seq and Pool-seq, and explore the potential of  
135 genotype imputation for bolstering inference with lcWGS data. Finally, in Sections 6 and 7, we  
136 review challenges and limitations associated with lcWGS data and discuss future perspectives.  
137 With this practitioner-centered overview, we hope to make lcWGS seem more approachable  
138 and stimulate broader adoption of this powerful approach, while inspiring future development of  
139 population genomic inference methods for lcWGS data.

140

141

## 142 **2. Feasibility: What does lcWGS cost and what resources are** 143 **required?**

144

### 145 **2.1 Current sequencing costs**

146 It is a widespread assumption that whole genome sequencing approaches are still too  
147 expensive for researchers working on modest budgets. Yet, due to spectacular drops in  
148 sequencing costs over the past decades (the cost per Mb of sequencing is today >600,000  
149 times cheaper than in 2000; (Wetterstrand, 2021), lcWGS can now - in many cases - be  
150 performed at similar per-sample costs as reduced-representation techniques. Table 1 provides  
151 estimates of the total per-sample cost for both library preparation and sequencing (based on  
152 November 2020 pricing) for organisms of different genome sizes. The cost of lcWGS inevitably  
153 scales with genome size (because more sequence data are needed to provide a target  
154 coverage level of a large vs. a small genome), and this approach therefore may remain  
155 impractical for organisms with extremely large genome sizes. However, even for organisms with  
156 sizeable genomes around 1 Gb (e.g. many birds, fish, invertebrates, and plants), the per-sample  
157 cost with 1-2x sequencing coverage (20-32 USD) is now on par with the 30 USD recently  
158 reported for genotyping 20,000 variable RAD-seq loci, 15 USD for a custom sequence capture  
159 approach for 500 - 10,000 loci (Meek & Larson, 2019) and 48 USD for custom exome capture  
160 (Puritz & Lotterhos, 2018). For organisms with smaller genome sizes, lcWGS can be cheaper  
161 than reduced-representation approaches, and prices are likely to drop further as sequencing  
162 costs continue to decrease.

163

164

### 165 **2.2. Library preparation**

166 Depending on target coverage levels, Pool-seq approaches remain the most cost-effective way  
167 to obtain genome-wide population-level data because it only requires preparation of a single  
168 sequencing library per population. The obvious downside is that all individual-level information is

169 lost, precluding many types of analysis. Despite this limitation, Pool-seq has gained popularity  
170 because preparation of separate indexed libraries for hundreds of individuals used to be labor-  
171 intensive and costly (the costs for preparing hundreds of libraries could easily outweigh the cost  
172 of sequencing). LcWGS has now become a viable alternative because of the development of  
173 cheap library preparation methods with efficient workflows that make it both practical and  
174 affordable to process hundreds of samples. (Nina Overgaard Therkildsen & Palumbi, 2017) for  
175 example, describe a robust easy-to-implement protocol based on reduced reaction volumes of  
176 Illumina's Nextera kit, which brings per-sample reagent costs down to ~8 USD (based on  
177 current reagent pricing). Several other protocols that stretch reagents in commercial kits reach  
178 similar price points (e.g. Gaio et al., 2019; Li et al., 2019). An advantage of commercial kit-  
179 based protocols is that they often work "straight out of the box" or require only limited  
180 optimization. Substantial further cost savings can be achieved with protocols based on in-house  
181 expression and purification of *tn5* transposase (the enzyme used in Illumina's Nextera  
182 tagmentation approach), such as described by Hennig et al., (2018) and Picelli et al., (2014).  
183 With those protocols, per-sample library costs can be brought to <<1 USD, substantially  
184 reducing overall project costs when analyzing hundreds of samples and essentially eliminating  
185 the added cost of individually indexed libraries, making total costs for LcWGS equivalent to Pool-  
186 seq for similar total sequencing effort per population.

187

188 LcWGS library preparation methods also tend to be very efficient and scalable. For example,  
189 tagmentation-based protocols (like the one used by Therkildsen & Palumbi 2017) make it  
190 possible to prepare 96 libraries in <5 hours (with <3 hours hands-on time) - substantially less  
191 time than needed for most RAD-seq protocols (Meek & Larson, 2019). The Therkildsen and  
192 Palumbi (2017) protocol also works well for relatively degraded DNA and requires only very  
193 small amounts of input DNA (~2.5 ng). For highly degraded DNA, we have had great success  
194 with the Carøe et al. (Carøe et al., 2018) single-tube method. Other cost-effective protocols  
195 produce successful LcWGS libraries even from picogram-levels of input DNA (Hennig et al.,  
196 2018; Meier, Salazar, Kučka, Davies, & Dréau, 2020; Picelli et al., 2014), for example enabling  
197 high throughput production of libraries from individual zooplankters (Beninde, Möst, & Meyer,  
198 2020). Methods that sidestep DNA extraction with tagmentation directly on cells or tissue may  
199 lead to additional efficiencies for LcWGS library preparation in the future (Vonesch et al., 2020).

200

201

### 202 **2.3. The need for a reference genome**

203 For non-model organisms, a key constraint associated with LcWGS is the need for a reference  
204 genome to map the short-read sequence data generated from each individual. If a reference  
205 genome is not already available for the species of interest, a common solution is to map to a  
206 reference genome of a related species. While this can work well in some contexts, increasing  
207 phylogenetic divergence between the re-sequenced species and the reference genome can  
208 restrict mapping to the genomic regions that are most conserved between the two taxa and bias  
209 estimates of population genomic parameters (Bohling, 2020; Nevado et al., 2014). Major  
210 differences in genome organization (e.g. structural and copy number variants) can also exist  
211 even between closely related species (Ekblom & Wolf, 2014). For these reasons, a species-  
212 specific reference sequence is preferable where it can be obtained.

213  
214 As a shortcut to obtaining species-specific reference sequence without de novo assembling a  
215 full genome, Therikildsen and Palumbi (2017) mapped lcWGS reads to a reference  
216 transcriptome, in practice performing ‘in-silico’ exome capture. However, major advances in  
217 affordable long-read sequencing, powerful genome scaffolding techniques, and improved  
218 assembly algorithms now enable chromosome-scale assemblies at a much lower cost and  
219 faster speed than earlier approaches (reviewed by Rice & Green, 2019), facilitating high-quality  
220 assemblies of mammalian-sized genomes (several Gb) with chromosome-length scaffolds for  
221 as little as 1,000 USD (Dudchenko et al., 2018; Gatter, von Löhneysen, Drozdova, Hartmann, &  
222 Stadler, 2020). Therefore, at this point, it probably makes sense to start most new lcWGS  
223 studies with a de novo genome assembly or upgrade, if a reference sequence of sufficient  
224 quality is not available.

225  
226

## 227 **BOX 1: Glossary**

228

229 **Bayesian inference:** a statistical inference strategy that estimates model parameters by  
230 characterizing its posterior probability distribution (i.e.  $P(\text{parameter} | \text{data})$ ). By the Bayes  
231 theorem, the posterior probability is formulated as a product of the likelihood function and the  
232 prior probability distribution (probability distribution of model parameters before considering the  
233 data) divided by the marginal probability of the data (which is a constant), i.e.  $P(\text{parameter} |$   
234  $\text{data}) = P(\text{data} | \text{parameter}) * P(\text{parameter}) / P(\text{data})$

235

236 **Genotype dosage:** the expected genotypic count. For diploid individuals, genotype dosage =  
237  $P(\text{AA} | \text{data}) * 0 + P(\text{AB} | \text{data}) * 1 + P(\text{BB} | \text{data}) * 2$ , where A and B represent the two alleles at the  
238 site, and e.g.  $P(\text{AB} | \text{data})$  represents the posterior probability of the heterozygous genotype.

239

240 **Genotype imputation:** A method to infer missing genotypes and bolster genotype likelihood  
241 estimation by identifying stretches of haplotypes shared between individuals.

242

243 **Genotype likelihoods (GLs):** the probability of observing the sequencing data at a certain site  
244 in an individual given that the individual has each of the possible genotypes at this site (e.g. for  
245 diploids there are 10 possible genotypes, which can be reduced to 3 if the major and minor  
246 alleles are known), i.e.  $P(\text{data} | \text{genotype})$ , or  $L(\text{genotype})$ .

247

248 **Genotype likelihood model:** the mathematical model used to estimate GLs. Different GL  
249 models are built under different assumptions about the data, in particular about the sequencing  
250 error profile. For example, the GATK model assumes that the sequencing quality scores  
251 accurately capture the probability of sequencing error, and that all errors are independent. In  
252 comparison, the Samtools model assumes that once a first error occurs at a certain site in an  
253 individual, subsequent errors are more likely.

254

255 **Low-coverage whole genome re-sequencing (lcWGS):** We use this term to refer to whole  
256 genome re-sequencing of individuals (i.e. labeled with unique barcodes) with depth too low to

257 reliably call genotypes without imputation (<5x). Note, however, that even for medium  
258 sequencing depth (5-20x), inference accuracy may improve under a probabilistic analysis  
259 framework based on GLs, rather than working with called genotypes (Nielsen et al., 2011).

260

261 **Maximum likelihood inference:** a statistical inference strategy that estimates model  
262 parameters by choosing the parameters that maximize the likelihood of the data. In other words,  
263 the maximum likelihood estimators of model parameters =  $\text{argmax}(L(\text{parameter}))$

264

265 **Posterior genotype probability:** the probability of an individual having one of the possible  
266 genotypes at a certain site given the sequencing data, i.e.  $P(\text{genotype} \mid \text{data})$ .

267

268 **Prior genotype probability:** the probability of an individual having one of the possible  
269 genotypes at a certain site before considering the sequencing data for this individual at this site,  
270 i.e.  $P(\text{genotype})$ . The prior genotype probability can be uniform (i.e. all genotypes are equally  
271 likely to occur), or can be informed by the allele frequency or the site frequency spectrum (SFS)  
272 at this site for all individual samples. It is often used for the estimation of posterior genotype  
273 probability in Bayesian inference.

274

275 **Restriction site-associated DNA sequencing (RAD-seq):** a group of techniques for  
276 sequencing short flanking regions around restriction enzyme cut sites to obtain random samples  
277 of genetic markers across the entire genome. These markers are typically sequenced at high  
278 depth (e.g. >20x) for each individual so that individual genotypes can be confidently determined.

279

280 **Sample allele frequency (SAF) likelihood:** the probability of observing sequencing data at a  
281 certain site across all individual samples given each possible sample allele frequency at this site  
282 (e.g. for diploids, the possible sample allele frequencies range from 0 to  $2n$ ;  $n$ =sample size), i.e.  
283  $P(\text{data} \mid \text{sample allele frequency})$ .

284

285 **Whole genome sequencing of pools of individuals (Pool-seq):** a whole genome sequencing  
286 strategy in which unlabeled DNA from multiple individuals is pooled before sequencing. The  
287 sequencing depth is typically low on a per-individual level but high for each pool (e.g. >50x).  
288 Due to the absence of individual barcodes, all individual-level information is lost in the  
289 sequencing data.

290

291

### 292 **3. The toolbox: What types of analysis can we do with low-coverage** 293 **data?**

294

295 The major challenge in working with lcWGS data is that individual genotypes cannot be  
296 accurately inferred (Li, Sidore, Kang, Boehnke, & Abecasis, 2011; Nielsen et al., 2012, 2011).  
297 Many analytical tools that incorporate the uncertainty about individuals have therefore been  
298 developed in recent years, covering the most common types of population genomic inference.  
299 We briefly introduce the most widely used applications (see Table 2 for a more comprehensive

300 list) and also provide a tutorial with example data as a starting point for exploration:  
301 <https://github.com/nt246/lcWGS-guide-tutorial>.

302  
303 Currently, the most widely used program for lcWGS analysis is ANGSD (Korneliussen,  
304 Albrechtsen, & Nielsen, 2014), a comprehensive package that implements an extensive variety  
305 of analysis options. Because of its broad use and versatility, ANGSD will feature prominently in  
306 this section's overview of available tools. However, we also seek to highlight that a variety of  
307 alternative programs are available for most types of analysis (Table 2).

308  
309

### 310 **3.1. Accounting for genotype uncertainty**

311 The most common way to incorporate uncertainty about true genotypes is to use genotype  
312 likelihoods (GLs) rather than genotype calls in downstream analyses. A GL reflects the  
313 probability of observing the sequencing reads that cover a specific site in an individual if said  
314 individual has a particular genotype at this site. GLs refer to the set of likelihoods computed for  
315 each of all possible genotypes that individual could hold at that site (e.g. for diploids there are  
316 ten possible genotypes: AA, AC, AG, AT, CC, CG, CT, GG, GT, and TT, which can be reduced  
317 to three possible genotypes if the major and minor allele at a site is known, i.e. major-major,  
318 major-minor, minor-minor.

319  
320 The key factors that prevent us from confidently identifying the true genotype with lcWGS data  
321 is uncertainty about 1) whether both alleles of a diploid individual have been sampled in the  
322 stochastic sequencing process, 2) whether the base call (A, C, G, T) at each position of a  
323 sequencing read is correct, and 3) whether sequencing reads have been mapped to the correct  
324 position in the genome. Several models for how we should account for these uncertainties in  
325 computing GLs from sequencing data have been proposed, with the main difference between  
326 current models is their assumptions about how base quality scores relate to the true  
327 probabilities of sequencing error (i.e. issue 2 above; see Supplementary text for more detail;  
328 Blischak, Kubatko, & Wolfe, 2018; Korneliussen et al., 2014; Kousathanas et al., 2017).  
329 Unfortunately, the effects of GL model choice on downstream analyses are still incompletely  
330 understood. While GL model choice has been suggested to make little difference for most  
331 downstream analyses, inference that depends on accurate detection of rare alleles can be more  
332 sensitive (Korneliussen et al., 2014). In general, the sensitivity to GL model choice may depend  
333 on the accuracy of base calling, read coverage distribution and filtering, sample size, and  
334 particular individuals included in the sample (see Box 4 in Fuentes-Pardo & Ruzzante, 2017). In  
335 Section 4.1, we report one example where the choice of GL model can strongly influence the  
336 number of low frequency SNPs estimated from simulated low coverage ( $\leq 2x$ ) data but more  
337 research is needed to compare the performance of these different models. In the meantime, it  
338 may be prudent to compare inference with several different models with a subset of the data for  
339 each new dataset, particularly for analyses that rely on rare alleles.

340  
341

342 **3.2. From raw reads to SNP identification**

343 The initial steps in processing lcWGS data are similar to those used in many other NGS  
344 approaches, such as high-coverage whole genome sequencing and Pool-Seq (Figure 2). These  
345 include trimming adapter sequence and bases with low quality scores, mapping (aligning) reads  
346 to a suitable reference genome, removing poorly mapped and duplicated reads, and optionally  
347 realigning reads that span indels (see e.g. Therkildsen & Palumbi 2017). It is in the downstream  
348 processing of the resulting filtered bam files that high-coverage and low-coverage workflows  
349 diverge and where a probabilistic framework based on GLs becomes central for low-coverage  
350 data.

351  
352 The optimal approach in a GL-based framework would arguably be to compute GLs for every  
353 site in the genome for all analysis, including sites that appear to be invariant in a sample  
354 (because with lcWGS data we cannot be completely confident that we have not missed an  
355 alternative allele in one or more of our samples). While this approach is required for some  
356 analysis (e.g. for estimation of the site frequency spectrum and related estimates of genetic  
357 diversity), other types of analysis are more tractable and computationally efficient if only  
358 polymorphic sites are considered. Thus, a more practical solution is to initially identify likely  
359 polymorphic sites and restrict most GL-based analyses to those sites.

360  
361 Although many types of genetic variants exist, lcWGS analysis is typically restricted to bi-allelic  
362 single-nucleotide polymorphisms (SNPs). A range of programs can identify SNPs from lcWGS  
363 data (Table 2). Because of built-in integration of a broad variety of downstream analysis tools,  
364 ANGSD is often a convenient option. ANGSD identifies SNPs as sites with minor allele  
365 frequencies significantly larger than zero. In this case, the number of alleles at each site is  
366 restricted to two (major and minor allele), with the identities of these alleles either determined  
367 through a maximum likelihood approach, setting the more common allele as the major allele  
368 (Jørsboe & Albrechtsen, 2019; Skotte, Korneliusen, & Albrechtsen, 2012) or by user  
369 specification (e.g. setting the reference or ancestral allele as the major allele). ANGSD currently  
370 does not allow for identification of indels or multi-nucleotide polymorphisms, but users could  
371 potentially identify biallelic indels with a different tool, such as Freebayes (Garrison & Marth,  
372 2012) or GATK (McKenna et al., 2010), and import estimated GLs into ANGSD for use in  
373 downstream analysis. Regardless of the program used, quality control filters can be crucial to  
374 ensure data reliability. Table 3 provides an overview of the key filters that should be considered  
375 for different types of analysis with lcWGS data.

376  
377

378 **3.3. Individual-level analyses**

379 Despite the lack of called genotypes, lcWGS data can be used for a wide range of individual-  
380 level analyses, which we define as those that do not require a priori grouping individual  
381 samples. It should be noted that the input formats for the different approaches differ between  
382 programs and that in some cases the SNP identification can be performed as part of the  
383 analyses (see specific manuals). Note also that none of the analyses listed in this subsection  
384 are possible with Pool-seq data.

385

386 **Population structure:** A key component of many population genomic studies is to characterize  
387 population structure, using dimensionality reduction (e.g. PCA and PCoA) and/or model-based  
388 clustering (e.g. admixture analysis). Dimensionality reduction methods are based on a  
389 covariance matrix (PCA) or distance matrix (PCoA). Several methods for computing these  
390 matrices while accounting for genotype uncertainty have been implemented. ANGSD, for  
391 example, can either randomly sample one read per individual per site or use the most common  
392 allele to represent the individual's allele frequency at this site (as either 0 or 1) and then  
393 calculate the covariance and distance between every pair of individuals from these allele  
394 frequencies. This simple approach has been shown to work well for datasets with very low  
395 sequencing depth and uneven coverage across samples (see section 4.2 and ANGSD  
396 manual). PCAngsd (Meisner & Albrechtsen, 2018), in contrast, estimates the covariance matrix  
397 from posterior genotype probabilities while correcting for potential violation of the Hardy-  
398 Weinberg equilibrium.

399

400 Model-based clustering methods that estimate admixture proportions of each sample assuming  
401 a model of discrete ancestral populations are also implemented in several software programs  
402 using GLs as input. These include NGSAdmix (Skotte, Korneliussen, & Albrechtsen, 2013) and  
403 Ohana (Cheng, Racimo, & Nielsen, 2019). They both adopt a maximum likelihood  
404 implementation of the classic STRUCTURE model, (Pritchard, Stephens, & Donnelly, 2000;  
405 Tang, Peng, Wang, & Risch, 2005), but differ in their optimization approaches. PCAngsd  
406 implements a different approach, which uses an intermediate output from its PCA analysis as a  
407 starting point for model-based clustering. PCAngsd has been shown to outperform NGSAdmix  
408 in runtime without strongly compromising its inference accuracy, making it potentially more  
409 suitable for larger datasets (Meisner & Albrechtsen, 2018).

410

411 **Selection scans:** Several of these clustering programs also implement selection scan  
412 approaches that do not require a priori grouping of individuals, as their general strategy is to  
413 locate outlier loci that exhibit patterns of genetic variation among individuals that are highly  
414 different from the genome-wide average. For example, PCAngsd (Meisner & Albrechtsen, 2018;  
415 Meisner, Albrechtsen, & Hanghøj, 2021) implements the FastPCA method by (Galinsky et al.,  
416 2016) in a GL framework and in Ohana, SNPs that exhibit a significantly different covariance  
417 structure can be identified as potentially under selection.

418

419 **Genome-wide association studies (GWAS):** Multiple statistical frameworks have been  
420 developed to take genotype uncertainty into account in scans for genotype-phenotype  
421 associations. GWAS often require large sample sizes to gain sufficient power, and a lcWGS/GL-  
422 based approach provides an opportunity to maximise the number of individuals studied in a  
423 cost-efficient way. Several GL-based GWAS approaches implemented in ANGSD have shown  
424 power to discover meaningful associations, including in the presence of population structure  
425 (Jørsboe & Albrechtsen, 2019; Skotte et al., 2012). These methods range from simple case /  
426 control associations for identifying variants associated with binary phenotypes (Kim et al., 2011)  
427 to the analyses of quantitative traits with incorporation of covariates (Skotte et al. 2012; Jørsboe  
428 & Albrechtsen 2019). The maximum likelihood approach recently developed by (Jørsboe &  
429 Albrechtsen, 2019) also explicitly estimates the effect size of each locus.

430

431 **Linkage disequilibrium (LD):** LD estimation has many important applications, for example  
432 relating to inference of population size, demographic history, selection, and discovery of  
433 structural variants (Slatkin, 2008). In addition, since many downstream analyses make  
434 assumptions about the independence of genomic loci, LD estimation is essential for pruning lists  
435 of loci to avoid inclusion of strongly linked loci. Several approaches have been developed to  
436 estimate LD from GLs (i.e. taking genotype uncertainty into account), with examples being  
437 GUS-LD (Bilton et al., 2018) and ngsLD (Fox, Wright, Fumagalli, & Vieira, 2019). Unfortunately,  
438 the computational complexity of GUS-LD is too high for it to be practical for whole genome data,  
439 but ngsLD has a more efficient algorithm and has different built-in functionalities to limit its  
440 computational complexity (e.g. restricting LD estimation between SNPs within a set distance,  
441 setting a minor allele frequency filter, etc.), and comparative evaluation has indicated that  
442 ngsLD tends to show less bias at low read depths (1-2x) than GUS-LD (Bilton et al., 2018; Fox  
443 et al., 2019).

444

445 **Other types of analysis:** In addition to the examples discussed above, many other specialized  
446 software packages have been developed to account for genotype uncertainty in various types of  
447 inference, including estimation of relatedness among individuals (Korneliussen & Moltke, 2015;  
448 Link et al., 2017), parentage inference (Whalen, Gorjanc, & Hickey, 2019) and pedigree analysis  
449 (Snyder-Mackler et al., 2016), estimation of individual inbreeding coefficients (Link et al., 2017;  
450 Vieira, Fumagalli, Albrechtsen, & Nielsen, 2013) and identity-by-descent tracts (Vieira,  
451 Albrechtsen, & Nielsen, 2016), tests for introgression such as computation of ABBA-BABA/D-  
452 statistic (Korneliussen et al., 2014), and construction of linkage maps (Rastas, 2017). More  
453 examples are listed in Table 2. It is also important to note that samples sequenced to low-  
454 coverage of the nuclear genome typically have very high sequencing depth across the  
455 mitochondrial genome due to its much higher copy number in each cell, enabling recovery of  
456 high-confidence full mitochondrial genome sequences for each individual (see e.g. Therkildsen  
457 & Palumbi 2017). LcWGS thus provides a cost-effective way to generate full mitochondrial  
458 genome sequences for hundreds of individuals, enabling unprecedented resolution for  
459 phylogeographic analysis (Lou et al., 2018; Margaryan et al., 2020).

460

461

### 462 **3.4. Population-level analyses**

463 When individual samples can be grouped into discrete populations or categories based on  
464 either prior information (e.g. sampling location or experimental treatment) or results from  
465 individual-level population structure analyses (e.g. model-based clustering), analyses can be  
466 conducted at the population level.

467

468 **Allele frequency estimation:** The estimation of population-specific allele frequencies is  
469 essential for most population genomic studies as it is a required input for many downstream  
470 analyses. Many programs, such as ANGSD or ATLAS, can estimate minor allele frequencies for  
471 each site using a maximum-likelihood or Bayesian approach (Kim et al., 2011; Kousathanas et  
472 al., 2017). Since population-specific estimates are obtained by running the program, e.g.  
473 ANGSD, on each population separately, it is crucial for users to explicitly define the same alleles

474 as major and minor in each population to avoid inadvertently computing the frequency of  
475 opposite alleles in different populations.

476  
477 **Site frequency spectrum (SFS):** The population-specific SFS is another population genomic  
478 parameter essential for many downstream analyses. A challenge in estimating the SFS with  
479 low-coverage data is that low-frequency SNPs are less likely to be identified as polymorphic and  
480 therefore an SFS directly estimated from allele frequencies at identified SNP positions can be  
481 biased towards intermediate frequencies. To get around this issue, ANGSD estimates the SFS  
482 by using the sample allele frequency (SAF) likelihoods to formulate the likelihood function of the  
483 SFS, which the program then optimizes (Nielsen et al., 2012). Depending on the availability of  
484 an outgroup or ancestral reference genome, the inferred SFS can either be folded or unfolded  
485 and ANGSD can estimate the SFS jointly for up to four populations (Nielsen et al., 2012). This  
486 approach can correct for the bias caused by low-coverage data, but its performance can be  
487 sensitive to the choice of underlying GL model (Korneliussen et al., 2014), also see Section  
488 4.1). Another important limitation is that the runtime of the algorithm currently implemented in  
489 ANGSD grows quadratically with the number of samples and it can become impractical to run  
490 across the whole genome if the sample size is very large. One strategy is to estimate SFS by  
491 chromosomes or in smaller windows and sum them up in the end. Implementation of a faster  
492 algorithm (Han, Sinsheimer, & Novembre, 2015) may also be included in future ANGSD  
493 releases (Fumagalli, personal communication).

494  
495 **Genetic diversity and neutrality test statistics within a single population:** Derived  
496 estimators for genome-wide genetic diversity  $\theta$ , such as nucleotide diversity  $\pi$  and Watterson's  
497 estimator, can be directly calculated from the population-specific SFS. These estimators of  $\theta$   
498 can also be computed within genomic windows from window-specific SFS and subsequently,  
499 different neutrality test statistics (e.g. Tajima's D) that evaluate the skewness of SFS in each  
500 genomic window can be calculated. Individual heterozygosity estimates can be obtained by  
501 estimating the SFS for individuals (rather than populations). All these diversity statistics can be  
502 computed based on an infinite sites model implemented in ANGSD. In contrast, ATLAS  
503 (Kousathanas et al., 2017) bases its  $\theta$  estimation on a model that allows for back mutations  
504 (Felsenstein, 1981), which can be more appropriate when working with ancient samples.  
505 Regardless of the method used, it is important to note that when generating diversity estimates,  
506 non-variable sites should be included in the calculation, and therefore minimum minor allele  
507 frequency filters or SNP p-value filters should not be used.

508  
509 **Genetic differentiation between populations:** In addition to estimates of *within*-population  
510 diversity, the genetic differentiation *between* populations can be estimated with a variety of  
511 different statistics, from simply quantifying the allele frequency difference to more complex  
512 statistics such as relative genetic differentiation ( $F_{ST}$ ) and absolute genetic divergence ( $d_{xy}$ ).  
513 Various estimators of  $F_{ST}$  can be computed from GL data using ANGSD, ngsTools (Fumagalli et  
514 al., 2013), or vcflib (see Supplementary text for more detail). vcflib can also estimate  $pF_{ST}$ , which,  
515 contrary to what the name suggests, is not an  $F_{ST}$  estimator, but a statistic that quantifies the  
516 significance of allele frequency differences between populations in face of genotype uncertainty  
517 (Domyan et al., 2016). In contrast to  $F_{ST}$ , no established method to estimate  $d_{xy}$  from GLs has, to

518 our knowledge, been included in major software packages. Various custom scripts have been  
519 shared (see e.g. <https://github.com/mfumagalli/ngsPopGen/tree/master/scripts>,  
520 [https://github.com/marqueda/PopGenCode/blob/master/dxy\\_wsfs.py](https://github.com/marqueda/PopGenCode/blob/master/dxy_wsfs.py)). Note, however, that  $d_{xy}$  may  
521 be over-estimated with these scripts so they should be used only for inspecting the relative  
522 distribution of  $d_{xy}$  across the genome (Foote et al., 2016) and not to make inferences based on its  
523 absolute values.

524  
525 **Other analyses based on derived statistics:** In addition to the methods that work directly with  
526 the GLs, many other types of population-level analysis can be conducted based on the derived  
527 statistics mentioned above. For example, several commonly used software tools can use allele  
528 frequency matrices as input to infer population relationships and potential gene flow (e.g.  
529 Treemix (Bradburd, Coop, & Ralph, 2018; Pickrell & Pritchard, 2012) and conStruct (Bradburd  
530 et al., 2018; Pickrell & Pritchard, 2012)), perform selection scans (e.g. BayPass or WFABC (Foll  
531 & Gaggiotti, 2008; Foll, Shim, & Jensen, 2015; Gautier, 2015)), association analyses (e.g.  
532 BayPass) or variance partitioning analyses (e.g. RDA (Forester, Lasky, Wagner, & Urban,  
533 2018)). To run these programs, population-level allele frequencies are estimated as explained  
534 above (e.g. using ANGSD), but have to be transformed into the appropriate input format using  
535 custom scripts. Similarly, the population-specific or multi-dimensional SFS estimated from  
536 ANGSD can be used to infer demographic history (e.g.  $\delta a \delta i$  (Excoffier & Foll, 2011; Gutenkunst,  
537 Hernandez, Williamson, & Bustamante, 2009), fastsimcoal2 (Excoffier & Foll, 2011; Gutenkunst  
538 et al., 2009)), or to explicitly control for the effect of demography in selection scans (e.g.  
539 SweepFinder2 (DeGiorgio, Huber, Hubisz, Hellmann, & Nielsen, 2016)). Both locus-specific  
540 neutrality test statistics and  $F_{ST}$  values can be used in selection scans (e.g. outFlnk (Whitlock &  
541 Lotterhos, 2015)), and genome-wide  $F_{ST}$  estimates can be used, for example, to test for  
542 isolation by distance (Mantel test) or to estimate effective migration surfaces (e.g. EEMS  
543 (Petkova, Novembre, & Stephens, 2016)). Furthermore, Ancestry\_HMM (Medina, Thornlow,  
544 Nielsen, & Corbett-Detig, 2018) and ancestryinfer (Schumer, Powell, & Corbett-Detig, 2020) can  
545 infer local ancestry across the genome without called genotypes, although they require detailed  
546 SNP information for reference populations. Using derived statistics as input data can be a  
547 powerful approach to expand the available toolbox for lcWGS. However, unlike the GL-based  
548 programs listed in the rest of this section and Table 2, this approach does not carry uncertainty  
549 about parameter estimation downstream. Accordingly, if summary statistics rather than GLs are  
550 used as input for analysis, p-values etc. should be interpreted with caution and in light of the  
551 expected precision given the sample size and sequencing depth (see section 4).

552  
553

#### 554 **4. Experimental design: The tradeoffs between sequencing depth per** 555 **sample and total number of samples analyzed**

556  
557 With a finite sequencing budget, do we learn more about a population from adding more  
558 sequencing depth to each individual or stretching the sequencing effort over more individuals?  
559 Several previous studies have used simulated data to address this question (e.g. Buerkle &  
560 Gompert, 2013; Fumagalli, 2013; Nevado et al., 2014). In general, these studies have found that

561 sampling many individuals at 1x or 2x read depth provides more accurate estimates of many  
562 population parameters than higher read depth for fewer individuals. However, both the  
563 simulation (e.g. Haller & Messer, 2019; Huang, Li, Myers, & Marth, 2012) and the GL-based  
564 data analysis toolboxes (e.g. Fumagalli, Vieira, Linderoth, & Nielsen, 2014; Korneliussen et al.,  
565 2014; Meisner & Albrechtsen, 2018) have evolved rapidly since these studies were conducted,  
566 and a more up-to-date evaluation is now needed. Here, we used simulated data to compare  
567 common types of population genomic inference under a wide range of sample size and  
568 sequencing depth combinations, including depths < 1x, which were not explicitly evaluated in  
569 earlier studies. Full details about all the simulations and analyses can be found in the  
570 supplementary methods and Table S2, and our entire simulation and analysis pipeline is  
571 available on GitHub (<https://github.com/therkildsen-lab/lcwgs-simulation>).

572  
573

#### 574 **4.1. Population genomic inference for single populations**

575 We simulated an isolated population that has reached mutation-drift equilibrium, and evaluated  
576 the accuracy of lcWGS in inferring key population genomic parameters, including allele  
577 frequencies, the SFS,  $\theta$ , Tajima's D, and linkage disequilibrium (LD) under different  
578 experimental designs (Fox et al., 2019; Haller & Messer, 2019; Huang et al., 2012; Korneliussen  
579 et al., 2014). As expected, more sequencing data is always better and the accuracy in allele  
580 frequency estimation consistently increases with both higher sample size and coverage (as  
581 measured by the  $r^2$  values in Figure 3). The number of false negative SNPs (i.e. true SNPs in  
582 the population that fail to be identified) similarly decreases with higher sample size and higher  
583 coverage (Figure S1). Importantly, however, distributing the same total sequencing effort (i.e.  
584 the product of sample size and coverage) across more samples, with each sample receiving  
585 lower coverage (i.e. going from bottom left to top right in Figure 3) also consistently improves  
586 allele frequency estimation, even when each sample is sequenced at a coverage as low as  
587 0.25x. This is because each allele is less likely to be sequenced more than once with lower per-  
588 sample coverage, and thus the effective sample size is higher.

589

590 Consistent with what the authors of ANGSD have previously shown (Korneliussen et al., 2014),  
591 we found that the GL model used for SFS-based inference can strongly influence its result. With  
592 the Samtools GL model, Watterson's  $\theta$  is systematically underestimated when the average  
593 coverage is low ( $\leq 4x$ ), although Tajima's  $\theta$  ( $\pi$ ) estimates are more robust (Figure S2).

594 Consequently, Tajima's D tends to be overestimated (Figure S3). In contrast, when the GATK  
595 GL model is used, Watterson's  $\theta$ , Tajima's  $\theta$ , and Tajima's D can all be accurately estimated  
596 even at coverage as low as 0.5x (Figure S2, S3). The two GL models differ in performance  
597 because both the GATK model and our simulation model assume that each base quality score  
598 reflects an independent and unbiased measurement of the probability of sequencing error  
599 (Huang et al., 2012; McKenna et al., 2010), whereas the Samtools model assumes that if one  
600 sequencing error occurs at a certain locus, subsequent errors are more likely (Li, 2011; Li et al.,  
601 2009). As a result, with the Samtools model, lower-frequency mutations are less likely to be  
602 identified as polymorphic sites and more likely to be interpreted as sequencing errors when the  
603 coverage is low. This leads to an underestimation of the number of singleton mutations, and  
604 therefore Watterson's  $\theta$  tends to be underestimated, at least for our simulated data. We note

605 that these low-frequency SNPs have minimal impact on many other population genomic  
606 analyses and, in fact, are often filtered out, so we do not expect strong discrepancies between  
607 the two GL models in most types of analysis. We also stress that the sequencing errors  
608 modeled in our simulations may not accurately represent the sequencing error profile in real life,  
609 so our result should not be interpreted as a recommendation of one GL model over the other.  
610

611 Lastly, we found that although relative estimates of LD (which may be adequate for many uses,  
612 e.g. for the identification of LD blocks or LD pruning) could reliably be obtained with per-sample  
613 coverage of 1-2x, higher per-sample coverage (e.g.  $\geq 4x$ ) would be required to get precise and  
614 accurate estimates of LD (e.g. for demographic inference) even with sample size as large as  
615 160 (Figure S4, S5, Fox et al. 2019).  
616  
617

## 618 **Box 2. Performance of lcWGS vs. Pool-seq in allele frequency** 619 **estimation**

620 A key advantage of lcWGS over Pool-seq is that each sequencing read can be assigned to an  
621 individual so we can detect uneven sequencing coverage and account for it in parameter  
622 estimation. But does it matter in practice when the contribution of each individual to the  
623 sequencing pool is roughly equal? With our simulated data, we found that a lcWGS analysis  
624 approach that accounts for individual-level GLs consistently provides slightly more accurate  
625 allele frequency estimates than Pool-seq analysis (which ignores individual-level information),  
626 even when the total amount of sequence is exactly equal for all individuals (Figure 4). This is  
627 because the sampling variance inherent to next-generation sequencing creates stochastic  
628 variation in the sequencing depth for each individual at each locus. In practice, inaccuracies due  
629 to measurement and pipetting errors, variation in DNA quality, and sequencing biases make it  
630 almost impossible to ensure the optimal scenario of even amounts of sequence among samples  
631 (Figure S6, Schlötterer, Tobler, Kofler, & Nolte, 2014), further enhancing the value of being able  
632 to account for sample overrepresentation with individually barcoded reads (Figure S7-S8).  
633  
634

### 635 **4.2. Inference of spatial structure**

636 To evaluate the power of different lcWGS sampling designs in detecting population structure,  
637 we simulated a metapopulation consisting of nine subpopulations located on a three-by-three  
638 grid that have reached mutation-drift-migration equilibrium. We first examined a scenario in  
639 which gene flow among subpopulations is low (0.25 effective migrants between neighboring  
640 subpopulations per generation). In this scenario, the spatial structure among subpopulations  
641 can be correctly inferred from PCA even with extremely low sample size (5 samples per  
642 subpopulation) and coverage (0.125x coverage per sample; Figure 5A). In addition, migrant  
643 individuals and hybrids, when included in the sample, can be identified in the PCA (Figure 5A),  
644 which would not be possible with a Pool-seq design.  
645

646 We then increased the level of gene flow (1 effective migrant between subpopulations every  
647 generation). As expected, the power of PCA to resolve the weaker spatial structure slightly  
648 declines, but interestingly, small sample size causes a greater loss of power than low coverage

649 does (Figure 5B). Subpopulations fail to form discrete clusters in the PCA space when the  
650 sample size per population is 5, unless the coverage is 2x or higher per sample. On the other  
651 hand, with a sample size of 10, the correct spatial structure can be inferred with a coverage as  
652 low as 0.125x (i.e. a per-population coverage of only 1.25x; Figure 5B). The reason we can  
653 push the per-sample coverage so low is that PCA depends on reliable covariance estimation  
654 between some, but not all pairs, of samples in the dataset. To get reliable covariance estimates  
655 in a sample pair, both samples need to have at least 1x coverage at some informative SNPs. As  
656 sample size increases, the number of all available sample pairs increases quadratically, and the  
657 number of sample pairs for which enough informative SNPs are shared also increases  
658 quadratically. Therefore, the overall population structure is more likely to be correctly  
659 extrapolated from these sample pairs. We also note that, due to computational limitations, our  
660 simulations are based on only a single 30Mb chromosome. Since the power of PCA depends on  
661 the number of informative SNPs shared between pairs of samples, with a larger genome size,  
662 even lower sequencing depth and/or sample size would be required to resolve the spatial  
663 structure among subpopulations, given the same SNP density as simulated here (see Figure S9  
664 for an example of this). Lastly, we found that ANGSD (Korneliussen et al., 2014), the results of  
665 which are presented here, outperforms PCAngsd (Meisner & Albrechtsen, 2018) in scenarios  
666 with low sample size (e.g.  $\leq 10$  samples per population) or very low coverage (e.g.  $\leq 0.25x$  per  
667 sample) (Figure S10-11).

668  
669

#### 670 **4.3. Scans for divergent selection in the face of gene flow**

671 A primary advantage of lcWGS compared to reduced-representation sequencing approaches is  
672 the increased resolution for genome scans for signatures of selection, for example in the form of  
673 outlier SNPs that show elevated levels of differentiation between populations. To evaluate how  
674 experimental design affects our ability to detect outliers, we simulated two populations  
675 connected by gene flow that are strongly affected by divergent selection. We estimated  $F_{ST}$   
676 between the two populations from lcWGS data to identify the loci under selection (details in the  
677 supplementary material).

678

679 We first examined a scenario where the size of each population is large ( $N_e = 5 \times 10^4$ ) and gene  
680 flow is high (5 effective migrants per generation). In this scenario, seven SNPs under divergent  
681 selection, along with their neighboring neutral SNPs, show highly elevated  $F_{ST}$  values compared  
682 to the genome-wide background, creating a distinct pattern of narrow genomic islands of  
683 divergence (Figure 6) (Turner, Hahn, & Nuzhdin, 2005). This  $F_{ST}$  landscape can be recovered  
684 from lcWGS data with a total sequencing coverage  $\geq 10x$  in each population (e.g. 40 samples  
685 per population and 0.25x coverage per sample, Figure 6). For a given total sequencing effort,  
686 however, we observe an increase in background  $F_{ST}$  when fewer samples are sequenced (e.g.  
687 40 samples each at 0.25x vs. 5 samples per population and 2x coverage per sample), which  
688 can lead to more false positive signals in the outlier detection (Figure 6). The same conclusions  
689 hold in a scenario with smaller  $N_e$  ( $N_e = 10^4$ ) and lower gene flow (2.5 effective migrants per  
690 generation) (Figure S12, S13).

691  
692

#### 693 4.4. The optimal experimental design depends on study goals

694 Perhaps unsurprisingly, our simulation results suggest that there is not a single lcWGS  
695 experimental design that is ideal for all purposes. Instead, the optimal design depends on the  
696 goals, system, and budget of a study. For many common types of population genomic inference  
697 (e.g. allele frequency estimation, population structure analysis, genetic differentiation between  
698 populations), higher accuracy can be achieved by spreading a given sequencing effort thinly  
699 across more samples (Figure 3, 5, 6). There are, however, some notable exceptions. For  
700 example, inference that depends heavily on low-frequency alleles (e.g. Watterson's  $\theta$ , Tajima's  
701 D) can be very sensitive to the chosen GL model when per-sample sequencing coverage is low,  
702 so until we have a better understanding of which GL models best fit the empirical data,  
703 sequencing each sample with relatively higher coverage (e.g. >4x) might generate more robust  
704 results for these types of analyses (Figure S2, S3). Similarly, the methods that are currently  
705 available for LD estimation with lcWGS data can generate biased estimates when the coverage  
706 is lower than 4x (Figure S4, S5), but note that reliable relative estimates of LD can be obtained  
707 at lower coverage.

708  
709 It is important to keep in mind that tradeoff exists between sample size and per-sample depth:  
710 with a given budget, the higher per-sample sequencing depth needed for robust estimation of  
711 the SFS (e.g. for demographic inference using  $\delta a \delta i$ ) or absolute values of e.g. Tajima's D or LD  
712 will likely compromise the accuracy for other estimates, e.g. of allele frequencies or  $F_{ST}$  outliers.  
713 Accordingly, researchers must carefully consider what types of inference are most essential to  
714 their study goals and strike an appropriate balance. Based on our results here and those from  
715 previous studies, we provide some general guidelines to lcWGS experimental design in Table 4.  
716 For more targeted guidance, we also encourage researchers to build on our simulation pipeline  
717 (<https://github.com/therkildsen-lab/lcwg-simulation>) to optimize the experimental design for  
718 their specific studies.

719  
720

#### 721 **Box 3. Performance of lcWGS vs. RAD-seq in selection scans**

722 Compared to lcWGS, RAD-seq has the advantage of being able to generate high-confidence  
723 genotype calls, but suffers from a sparser coverage of the genome, which can result in missed  
724 signals in selection scans (Lowry et al., 2017). Here, we simulated RAD-seq data for our two  
725 divergent selection scenarios with a range of realistic sample sizes and RAD tag densities. In  
726 the scenario with larger population size and higher gene flow, we found that even with a large  
727 sample size and a much higher marker density than typically used (128 RAD tags per Mb),  
728 RAD-seq picked up some, but tended to miss several of the narrow  $F_{ST}$  peaks. With a lower,  
729 much more commonly used marker density (e.g. 8 tags per Mb), the majority of the selection-  
730 induced peaks would be missed, regardless of sample size (Figure 7). In the scenario where the  
731 population size is smaller and gene flow is lower, RAD-seq is more likely to sample SNPs within  
732 the true  $F_{ST}$  peaks due to the stronger linked selection, but because of the higher background  
733 noise in these scenarios, it still struggles to detect distinct  $F_{ST}$  peaks (Figure S14). These  
734 findings are consistent with a growing number of empirical examples where RAD-seq missed  
735 signatures of selection clearly detected with WGS data (see introduction).

736

737

## 738 **5. Application to empirical data**

739

740 To supplement our simulation-based evaluation of lcWGS inference with an exploration of how  
741 sequencing depth affects the identification of polymorphic sites, population structure analysis  
742 and detection of outlier loci in empirical data, we subsampled and re-analysed previously  
743 published whole genome sequencing data from the Neotropical butterfly *Heliconius erato* (Van  
744 Belleghem et al., 2017). The *H. erato* radiation comprises several subspecies that show a vast  
745 visual diversity in Müllerian mimicry related to wing patterns, and many of the underlying  
746 candidate genes have been identified (Reed et al., 2011; Van Belleghem et al., 2017). For  
747 example, the *optix* gene has been shown to control the red band phenotype in multiple  
748 *Heliconius* species and accordingly shows strong differentiation among subspecies with  
749 different band patterns (Reed et al., 2011; Van Belleghem et al., 2017). We subsampled  
750 resequencing data (originally average coverage of  $11x \pm 2.3x$  per individual) mapped to the *H.*  
751 *erato demophoon* (v1) to coverage depths of 8x, 4x, 2x, 1x, 0.5x and 0.25x (see supplementary  
752 text) and analysed them in a GL framework. For simplicity, we focus on results for 8x, 2x and  
753 0.5x coverage, as results from 4x and 1x are very similar to 8x and 2x, respectively (see  
754 supplementary Figure S15).

755

756 First, we found a positive correlation between the number of variable sites identified during SNP  
757 identification in ANGSD and the mean genome-wide sequencing coverage (Figure 8a; quadratic  
758 function:  $r^2 = 0.98$ ,  $p=0.00099$ ). Across all 51 individuals used in the final analyses, the number  
759 of SNPs identified with a p-value threshold of  $1e-6$  ranged from 12,266 at 0.5x coverage to  
760 14,851,731 at a mean coverage depth of 8x. It has to be noted though, that the number of  
761 detected SNPs depends on the p-value threshold, and for a dataset with a mean per-individual  
762 coverage of 0.25x a lower p-value threshold would have to be used to identify any SNPs at all  
763 (Figure 8).

764

765 Second, we reconstructed the population structure using PCA, performed on covariance  
766 matrices estimated using random read sampling in ANGSD (see supplementary methods). The  
767 PCA showed a very similar clustering pattern for all datasets regardless of coverage level, with  
768 populations grouping into three distinct clusters corresponding to the geographic origin of  
769 samples (Central America, East of Andes, West of Andes; Figure 8b). One subspecies (*H. erato*  
770 *hydara*) sampled from two geographic regions was split over two clusters. On a finer population  
771 structure scale, we observed a slightly wider spread of data points at the lowest coverage  
772 (0.5x), although the general clustering was comparable to higher coverages.

773

774 Lastly, comparing the genetic differentiation between *H. erato* subspecies with ( $n=28$ ) and  
775 without ( $n=23$ ) the red bar phenotype (Van Belleghem et al., 2017), we recovered the well-  
776 characterized  $F_{ST}$  peak around the *optix* gene at per-individual coverages as low as 1x (Figure  
777 8c) (Van Belleghem et al., 2017). At 0.5x coverage, we were restricted to estimating  $F_{ST}$  within  
778 fewer genomic windows compared to higher coverages (112 50kb windows at 0.5x vs 255 50kb  
779 windows at  $>1x$  along scaffold 1801), leading to much sparser window coverage across the  
780 scaffold and therefore a noisier signal (Figure 8c). However, even at this low resolution, we

781 detected one differentiated genomic window in the optix region, albeit the estimated  $F_{ST}$  was  
782 elevated at 0.5x ( $F_{ST} \sim 0.6$ ) compared to higher coverages ( $F_{ST} \sim 0.4$ ).

783  
784 Overall, these results suggest that even at a comparatively low individual sequencing coverage  
785 of 0.5-1x and moderate sample sizes of 20-30 per population, we can detect population  
786 structure and recover distinct peaks of differentiation across the genome in empirical data.

787  
788

#### 789 **Box 4. Using imputation to bolster genotype estimation from lcWGS**

790

791 The majority of current population genomic inference methods, including all the lcWGS methods  
792 discussed in this paper so far, consider data on a SNP-by-SNP basis and accordingly ignore all  
793 the information contained in the surrounding haplotype structure. Imputation can be used to  
794 boost genotyping accuracy by leveraging LD patterns between variants to identify shared  
795 stretches of chromosome and incorporate information from flanking alleles to infer missing or  
796 low-confidence genotypes (Li et al., 2011; Pasaniuc et al., 2012). Imputation has been used  
797 extensively to obtain genotype calls from low-coverage data in humans and agricultural species,  
798 but has seen limited application in non-model species because most imputation methods, such  
799 as Beagle and findhap (Browning & Yu, 2009; VanRaden, Sun, & O'Connell, 2015), rely on  
800 externally generated haplotype reference panels, which are unavailable for most species. In  
801 contrast, the more recently developed program STITCH imputes directly from sequence read  
802 data without reference panels, and has been shown to perform well when sample sizes are  
803 large ( $n > 2000$ ; (Davies, Flint, Myers, & Mott, 2016). However, sample sizes of this magnitude  
804 are not achievable in many studies, especially for rare or elusive species. To evaluate the utility  
805 of imputation without reference panels with sample sizes more typical of studies of non-model  
806 species, we simulated three populations with varying levels of genetic diversity and LD, tested  
807 combinations of sequencing depths and sample sizes, and identified the conditions under which  
808 reference panel-free imputation is likely to bolster genomic analyses of lcWGS data.

809

#### 810 **Imputed genotype accuracy**

811 We simulated three populations characterized by 1) low diversity, high LD ( $N_e = 1,000$ ,  $r = 0.5$   
812 cM/Mb); 2) medium diversity, medium LD ( $N_e = 10,000$ ,  $r = 0.5$  cM/Mb); and 3) medium  
813 diversity, low LD ( $N_e = 10,000$ ,  $r = 2.5$ ). For each population, we subsampled 25, 100, 250, 500  
814 or 1000 individuals and simulated sequence reads to average depths of 1x, 2x and 4x per  
815 sampled individual. We compared genotype dosages for all SNPs with minor allele  
816 frequency  $> 0.05$  imputed without reference panels in Beagle v.3.3.2 and STITCH v.3.6.2, to  
817 those estimated without imputation in ANGSD v.0.931 (see the supplementary text and Table  
818 S2 for details on simulations, genotype dosage estimation and imputation).

819

820 Our analysis suggests that using imputation without reference panels does improve population  
821 genomic inference under certain circumstances. Imputation was most effective under the low  
822 diversity, high LD scenario (Figure 9A). Under this scenario, genotype dosages imputed in  
823 STITCH from large sample sizes ( $n \geq 500$ ) sequenced at 1x coverage were highly correlated with  
824 true genotypes ( $r^2 > 0.94$ ), and all experimental designs with sample sizes  $\geq 100$  showed a

825 substantial improvement in genotype estimation (Figure 9A). In the medium diversity and  
826 medium LD population, larger sample sizes were necessary to achieve similar imputation  
827 accuracy (e.g.,  $n=1000$  was needed for  $r^2=0.95$ ; Figure 9B). Performance was markedly worse  
828 in the populations with medium diversity, low LD, but there was nonetheless an improvement  
829 when imputing from large sample sizes ( $n \geq 250$ ) or greater sequencing depths ( $\geq 2x$ ) compared  
830 to genotypes called without imputation (Figure 9C).

831

### 832 **Considerations for using imputation in non-model systems**

833 Choosing whether to apply imputation to real-world data will depend on the details of the study  
834 system and the experimental design. In general, imputation accuracy increases with SNP  
835 density and LD between SNPs (de Bakker, Neale, & Daly, 2010; Shi et al., 2018), and our  
836 results suggest that populations with lower LD (even those with greater SNP density) require  
837 greater sample sizes and/or coverage to achieve the same imputation accuracy. For  
838 populations with higher LD, STITCH can substantially boost genotype accuracy for samples  
839 sequenced at 1x coverage, provided sample sizes are adequate ( $n \geq 100$ ). When coverage is  
840 higher ( $\geq 2x$ ), Beagle tends to perform similarly to or even outperform STITCH. However, for  
841 populations with lower LD, the improvement in genotype accuracy by imputation may be small  
842 unless sample sizes are  $\geq 1000$  and/or coverage is  $\geq 2x$  for the conditions tested here; at smaller  
843 sample sizes or lower coverage, the potential benefit of imputation for low LD populations may  
844 not warrant the computational time.

845

846 Imputation provides another potential benefit for spreading sequencing effort thinly among many  
847 individuals in some circumstances. As our results have shown, by leveraging LD information  
848 from all samples, imputation can to some extent make up for the genotype uncertainty inherent  
849 in lcWGS data. For example, in the high LD population, genotypes imputed in STITCH from  
850 1000 samples sequenced at 1x coverage were only slightly lower in accuracy ( $r^2=0.975$ ) than for  
851 500 samples at 2x coverage ( $r^2=0.981$ ) and 250 samples at 4x coverage ( $r^2=0.982$ ). For many  
852 questions where a large sample size is necessary to achieve adequate power, such as GWAS,  
853 what can be gained from increased sample size could readily outweigh the minimal loss in  
854 genotype accuracy. In addition, for some GWAS methods, the remaining genotype uncertainty  
855 can be incorporated directly into the analysis (Skotte et al., 2012; Jørsboe & Albrechtsen, 2019).

856

857 Because the performance of imputation varies with the LD and diversity of populations, a priori  
858 information on population history may help researchers anticipate how well imputation will  
859 perform. A set of “true genotypes” (e.g. from high-depth samples) and quality metrics output by  
860 the imputation programs (Browning & Yu, 2009; Davies et al., 2016) can also be used.

861 Populations with small  $N_e$  or that have experienced recent bottlenecks, such as threatened or  
862 endangered species, will have higher genome-wide LD (Hayes, Visscher, McPartlan, &  
863 Goddard, 2003; Waples & Do, 2010), making them potentially good systems for applying  
864 imputation if relatively large sample sizes (e.g.  $\geq 100$  for the scenarios simulated here) can be  
865 obtained. Where pedigree information is available, methods that incorporate the pedigree into  
866 imputation can be used (e.g. Ros-Freixedes, Whalen, Gorjanc, Mileham, & Hickey, 2020;  
867 Whalen, Ros-Freixedes, Wilson, Gorjanc, & Hickey, 2018). Finally, although imputation has  
868 been mainly applied to regular short-read data, the haplotype reconstruction step could be

869 greatly simplified by long-read or linked-read data that is becoming increasingly available (see  
870 section 7).

871

872

## 873 **6. Current limitations and future developments**

874

875 Despite the many strengths of lcWGS, there are also clear limitations to this data type. Here, we  
876 outline key constraints that researchers should consider before adopting the approach and  
877 discuss prospects for overcoming these constraints in the future.

878

879 **Not suitable for analysis requiring genotype calls:** It is important to stress that the potential  
880 for improved inference accuracy by spreading sequencing effort thinly over many individuals is  
881 only realized if the resulting uncertainty about individual genotypes is accounted for statistically  
882 in downstream analyses, with approaches such as those reviewed in section 3. As discussed,  
883 hard-calling genotypes from lcWGS data remains likely to bias inference regardless of how  
884 large the sample size is, so lcWGS data is not well-suited for analysis types or downstream  
885 software that require genotypes as input, unless imputation can provide more accurate  
886 genotype calls (see Box 4 for details). However, as outlined in section 3, GL-based inference  
887 frameworks are available for most major types of population genomic analysis and many  
888 additional approaches are under development.

889

890 **Lack of user-friendly interface and documentation:** Unfortunately, a key barrier to the wider  
891 adoption of lcWGS has been a lack of user-friendly interfaces and sparse documentation for  
892 programs that handle GL data. Accordingly, these tools are only accessible to users with prior  
893 expertise in bioinformatics, and the development of workflows often requires a substantial time  
894 investment. We hope that this beginner's guide can be part of the effort to increase the  
895 accessibility of lcWGS We are also aware that efforts are underway to develop a graphical front-  
896 end to ANGSD, which should make this powerful and versatile software package accessible to a  
897 broader set of researchers (Fumagalli, pers. comm).

898

899 **Computational demands:** Another practical limitation is the often much greater computational  
900 cost of GL-based methods compared to genotype-based methods. For example, SFS  
901 estimation from GLs in ANGSD is computationally intensive with very large sample sizes, which  
902 may be prohibitive for researchers without access to high-performance computational  
903 resources. New, more efficient algorithms (e.g. Han et al., 2015) and strategies for analyzing  
904 smaller sections of the genome in turn (see section 3) may alleviate some of these constraints,  
905 but the computational demands for analysis should definitely be considered, especially for  
906 researchers transitioning to lcWGS after working with much smaller datasets such as RADseq.

907

908 **Flaws and gaps in the current toolbox:** Although tremendous progress has been made in the  
909 development of methods and tools for the analysis of lcWGS data over the past decade, some  
910 key analytical challenges remain. One important issue is the potential sensitivity to the choice of  
911 GL model in some types of analyses (see sections 4.1 and Box 4 in Fuentes-Pardo & Ruzzante,  
912 2017). A better understanding of which GL models best match the real error structures

913 generated by different sequencing platforms is essential for more robust inference from low-  
914 coverage data. In addition, alignment error is not taken into account in any of the current GL  
915 models, which could be problematic for genomes with high repeat content or for poor-quality  
916 reference genomes. The current analysis framework implemented in most software packages is  
917 also centered on the analysis of diploid organisms; extension to an arbitrary ploidy level would  
918 expand its usefulness for working with haploid and polyploid organisms, and key parts of this  
919 framework have already been developed (Blischak et al., 2018). There also remain types of  
920 analysis for which GL-based methods are not yet available. However, new analytical  
921 approaches for lcWGS data also continue to emerge. GL-based equivalents to some  
922 established approaches, such as implementation of the Pairwise Sequentially Markovian  
923 Coalescent (PSMC) model, are currently under development (ngsPSMC  
924 [\[https://github.com/ANGSD/ngsPSMC\]](https://github.com/ANGSD/ngsPSMC)).

925  
926 **Analysis susceptible to batch artifacts:** LcWGS data have great potential for reusability  
927 because the possibility to combine different datasets does not depend on the selection of the  
928 same restriction enzyme or markers. However, lcWGS could be particularly susceptible to batch  
929 effects when different datasets are combined. As mentioned earlier, some GL-based  
930 approaches are heavily dependent on the accurate modeling of the error structure in the data,  
931 which can vary between sequencing batches. For example, the sequencing error could be  
932 overestimated in one batch and underestimated in another (Lou et al. in prep), leading to  
933 artificial differences between batches that could confound real biological signals. Many of these  
934 batch effects can be mitigated with simple bioinformatic approaches, although extra care needs  
935 to be taken (Lou et al. in prep).

936  
937 **Limited ability to phase lcWGS data:** A major limitation is that no bioinformatic solution is yet  
938 available to allow accurate phasing of lcWGS data without a reference panel, therefore  
939 prohibiting haplotype-based analyses. Haplotype data are a rich source of information, e.g. for  
940 inference of local ancestry tracks across the genome, demographic histories, or ongoing  
941 selective sweeps (see Leitwein, Duranton, Rougemont, Gagnaire, & Bernatchez, 2020) for a  
942 detailed overview). Despite major technological advances, long-read sequencing that can  
943 recover haplotype information remains too costly for typical population genomic studies.  
944 However, the recent development of an affordable linked-read low-coverage sequencing  
945 approach (Meier et al., 2020) promises to open many new opportunities for haplotype-based  
946 inference on a population scale by enabling efficient phasing and imputation of low-coverage  
947 linked-read data without a reference panel. Phased haplotype data will provide substantial  
948 improvement in imputation performance compared to the short-insert lcWGS data explored in  
949 Box 4, and make completely new types of analysis possible with lcWGS data.

950  
951 **Limitations for small sample sizes and very large genomes:** LcWGS will not be an optimal  
952 solution for all study systems. In particular, for species that are rare or difficult to collect (e.g.  
953 endangered or elusive species), it may be impossible to obtain adequate sample sizes for  
954 accurately estimating population genomic parameters with lcWGS (see section 4). In these  
955 cases, many types of analysis, such as demographic history, diversity, selective sweeps and  
956 inbreeding levels, can be performed based on deep sequencing of the genome of a few or even

957 just a single individual (e.g. Li & Durbin, 2011). For species with extremely large genomes (e.g.  
958 many amphibians and pine species), whole genome sequencing may also remain impractical at  
959 any sequencing depth from a cost or data storage/handling perspective, and reduced  
960 representation approaches such as RAD-seq or targeted sequence capture may be preferable  
961 (Burgon et al., 2020; McCartney-Melstad, Mount, & Shaffer, 2016). For targeted methods like  
962 sequence capture, low-coverage sequencing of larger sample sizes and associated GL-based  
963 analysis can, similar to WGS, confer distinct advantages over sequencing fewer individuals at  
964 higher depth (e.g. Snyder-Mackler et al., 2016; Nina O. Therkildsen et al., 2019; Warmuth &  
965 Ellegren, 2019; Wilder et al., 2020).

966  
967

## 968 **7. Conclusion**

969 In conclusion, although some limitations still exist for the use of lcWGS, this approach offers  
970 many advantages over reduced-representation sequencing or pooled WGS approaches and is  
971 ripe for broader implementation. We are excited about how its cost-effectiveness democratizes  
972 population-scale whole genome analysis, which until recently was only available to well-funded  
973 research groups working on model species. The ability to obtain full genome data for hundreds  
974 of individuals even on modest research budgets, and the rapidly expanding toolbox for versatile  
975 analysis of lcWGS data now makes it an increasingly promising approach for molecular ecology,  
976 conservation and evolutionary biology research. We hope this guide will inspire broader  
977 adoption to expedite the exploration of genomic variation across the tree of life.

978  
979

## 980 **Acknowledgements**

981 We would like to thank the Therkildsen Lab at Cornell University for comments on an earlier  
982 version of this manuscript, Philipp Messer and Robbie Davies for advice on analysis, the  
983 science Twitter community for help compiling the list of studies using lcWGS, and Matt Hare,  
984 Matteo Fumagalli, Andy Foote, Claire Mérot, one anonymous reviewer, and the editor for helpful  
985 comments on earlier versions of this manuscript. This study was funded through a National  
986 Science Foundation grant to NOT (OCE-1756316).

987  
988

## 989 **Data availability**

990 All scripts used to generate the analysis presented in this manuscript will be available in a  
991 GitHub repository release deposited in Zenodo. The NCBI SRA accession numbers for the  
992 Heliconius data re-analyzed in this project is available in Table S3.

993  
994

## 995 **Author contributions**

996 NOT conceived of the project. All the authors designed the research jointly and collaborated to  
997 compile the overview of available methods. RNL simulated the test data and performed the  
998 comparative analysis for different experimental designs, AJ performed the analysis of the

999 empirical data and designed the graphics, and APW performed the imputation analysis. All the  
1000 authors provided input on all analyses and wrote the manuscript together.  
1001

## References

- 1003 Aguilon, S. M., Campagna, L., Harrison, R. G., & Lovette, I. J. (2018). A flicker of hope:  
 1004 Genomic data distinguish Northern Flicker taxa despite low levels of divergenceLos  
 1005 taxones de *Colaptes auratus* son diferenciables con datos genómicos pese a sus bajos  
 1006 niveles de divergenciaGenomic data distinguish Northern Flicker taxa. *The Auk*, *135*(3),  
 1007 748–766.
- 1008 Aguilon, S. M., Walsh, J., & Lovette, I. J. (2020). Extensive hybridization reveals multiple  
 1009 coloration genes underlying a complex plumage phenotype. *bioRxiv*. Retrieved from  
 1010 <https://www.biorxiv.org/content/10.1101/2020.07.10.197715v1.abstract>
- 1011 Alex Buerkle, C., & Gompert, Z. (2013). Population genomics based on low coverage  
 1012 sequencing: how low should we go? *Molecular Ecology*, *22*(11), 3028–3035.
- 1013 Anderson, E. C., Skaug, H. J., & Barshis, D. J. (2014). Next-generation sequencing for  
 1014 molecular ecology: a caveat regarding pooled samples. *Molecular Ecology*, *23*(3), 502–512.
- 1015 Andrews, K. R., Good, J. M., Miller, M. R., Luikart, G., & Hohenlohe, P. A. (2016). Harnessing  
 1016 the power of RADseq for ecological and evolutionary genomics. *Nature Reviews. Genetics*,  
 1017 *17*(2), 81–92.
- 1018 Beninde, J., Möst, M., & Meyer, A. (2020). Optimized and affordable high-throughput  
 1019 sequencing workflow for preserved and nonpreserved small zooplankton specimens.  
 1020 *Molecular Ecology Resources*. doi: 10.1111/1755-0998.13228
- 1021 Bilton, T. P., McEwan, J. C., Clarke, S. M., Brauning, R., van Stijn, T. C., Rowe, S. J., & Dodds,  
 1022 K. G. (2018). Linkage Disequilibrium Estimation in Low Coverage High-Throughput  
 1023 Sequencing Data. *Genetics*, *209*(2), 389–400.
- 1024 Blischak, P. D., Kubatko, L. S., & Wolfe, A. D. (2018). SNP genotyping and parameter  
 1025 estimation in polyploids using low-coverage sequencing data. *Bioinformatics*, *34*(3), 407–  
 1026 415.
- 1027 Bohling, J. (2020). Evaluating the effect of reference genome divergence on the analysis of  
 1028 empirical RADseq datasets. *Ecology and Evolution*, *10*(14), 7585–7601.
- 1029 Bradburd, G. S., Coop, G. M., & Ralph, P. L. (2018). Inferring Continuous and Discrete  
 1030 Population Genetic Structure Across Space. *Genetics*, *210*(1), 33–52.
- 1031 Browning, B. L., & Yu, Z. (2009). Simultaneous Genotype Calling and Haplotype Phasing  
 1032 Improves Genotype Accuracy and Reduces False-Positive Associations for Genome-wide  
 1033 Association Studies. *American Journal of Human Genetics*, *85*(6), 847–861.
- 1034 Burgon, J. D., Vieites, D. R., Jacobs, A., Weidt, S. K., Gunter, H. M., Steinfartz, S., ... Elmer, K.  
 1035 R. (2020). Functional colour genes and signals of selection in colour-polymorphic  
 1036 salamanders. *Molecular Ecology*, *29*(7), 1284–1299.
- 1037 Campagna, L., Gronau, I., Silveira, L. F., Siepel, A., & Lovette, I. J. (2015). Distinguishing noise  
 1038 from signal in patterns of genomic divergence in a highly polymorphic avian radiation.  
 1039 *Molecular Ecology*, *24*(16), 4238–4251.
- 1040 Campagna, L., Repenning, M., Silveira, L. F., Fontana, C. S., Tubaro, P. L., & Lovette, I. J.  
 1041 (2017). Repeated divergent selection on pigmentation genes in a rapid finch radiation.  
 1042 *Science Advances*, *3*(5), e1602404.
- 1043 Carøe, C., Gopalakrishnan, S., Vinner, L., Mak, S. S. T., Sinding, M. H. S., Samaniego, J. A., ...  
 1044 Gilbert, M. T. P. (2018). Single-tube library preparation for degraded DNA. *Methods in  
 1045 Ecology and Evolution / British Ecological Society*, *9*(2), 410–419.
- 1046 Cheng, J. Y., Racimo, F., & Nielsen, R. (2019). Ohana: detecting selection in multiple  
 1047 populations by modelling ancestral admixture components. doi: 10.1101/546408
- 1048 Clucas, G. V., Kerr, L. A., Cadrin, S. X., Zemeckis, D. R., Sherwood, G. D., Goethel, D., ...  
 1049 Kovach, A. I. (2019). Adaptive genetic variation underlies biocomplexity of Atlantic Cod in  
 1050 the Gulf of Maine and on Georges Bank. *PLOS ONE*, *14*(5), e0216992.

1051 Clucas, G. V., Lou, R. N., Therkildsen, N. O., & Kovach, A. I. (2019). Novel signals of adaptive  
1052 genetic variation in northwestern Atlantic cod revealed by whole-genome sequencing.  
1053 *Evolutionary Applications*, 12(10), 1971–1987.

1054 Davey, J. W., Hohenlohe, P. A., Etter, P. D., Boone, J. Q., Catchen, J. M., & Blaxter, M. L.  
1055 (2011). Genome-wide genetic marker discovery and genotyping using next-generation  
1056 sequencing. *Nature Reviews. Genetics*, 12(7), 499–510.

1057 Davies, R. W., Flint, J., Myers, S., & Mott, R. (2016). Rapid genotype imputation from sequence  
1058 without reference panels. *Nature Genetics*, 48(8), 965–969.

1059 de Bakker, P. I. W., Neale, B. M., & Daly, M. J. (2010). Meta-analysis of genome-wide  
1060 association studies. *Cold Spring Harbor Protocols*, 2010(6), db.top81.

1061 DeGiorgio, M., Huber, C. D., Hubisz, M. J., Hellmann, I., & Nielsen, R. (2016). SweepFinder2:  
1062 increased sensitivity, robustness and flexibility. *Bioinformatics*, 32(12), 1895–1897.

1063 Domyan, E. T., Kronenberg, Z., Infante, C. R., Vickrey, A. I., Stringham, S. A., Bruders, R., ...  
1064 Shapiro, M. D. (2016). Molecular shifts in limb identity underlie development of feathered  
1065 feet in two domestic avian species. *eLife*, 5, e12115.

1066 Dudchenko, O., Shamim, M. S., Batra, S. S., Durand, N. C., Musial, N. T., Mostofa, R., ...  
1067 Aiden, E. L. (2018). The Juicebox Assembly Tools module facilitates de novo assembly of  
1068 mammalian genomes with chromosome-length scaffolds for under \$1000 (p. 254797). doi:  
1069 10.1101/254797

1070 Ekblom, R., & Wolf, J. B. W. (2014). A field guide to whole-genome sequencing, assembly and  
1071 annotation. *Evolutionary Applications*, 7(9), 1026–1042.

1072 Excoffier, L., & Foll, M. (2011). fastsimcoal: a continuous-time coalescent simulator of genomic  
1073 diversity under arbitrarily complex evolutionary scenarios. *Bioinformatics*, 27(9), 1332–  
1074 1334.

1075 Felsenstein, J. (1981). Evolutionary trees from DNA sequences: a maximum likelihood  
1076 approach. *Journal of Molecular Evolution*, 17(6), 368–376.

1077 Foll, M., & Gaggiotti, O. (2008). A genome-scan method to identify selected loci appropriate for  
1078 both dominant and codominant markers: a Bayesian perspective. *Genetics*, 180(2), 977–  
1079 993.

1080 Foll, M., Shim, H., & Jensen, J. D. (2015). WFABC: a Wright Fisher ABC-based approach for  
1081 inferring effective population sizes and selection coefficients from time-sampled data.  
1082 *Molecular Ecology Resources*, 15(1), 87–98.

1083 Foote, A. D., Vijay, N., Ávila-Arcos, M. C., Baird, R. W., Durban, J. W., Fumagalli, M., ... Wolf, J.  
1084 B. W. (2016). Genome-culture coevolution promotes rapid divergence of killer whale  
1085 ecotypes. *Nature Communications*, 7, 11693.

1086 Forester, B. R., Lasky, J. R., Wagner, H. H., & Urban, D. L. (2018). Comparing methods for  
1087 detecting multilocus adaptation with multivariate genotype-environment associations.  
1088 *Molecular Ecology*, 27(9), 2215–2233.

1089 Fox, E. A., Wright, A. E., Fumagalli, M., & Vieira, F. G. (2019). ngsLD: evaluating linkage  
1090 disequilibrium using genotype likelihoods. *Bioinformatics*, 35(19), 3855–3856.

1091 Fuentes-Pardo, A. P., & Ruzzante, D. E. (2017). Whole-genome sequencing approaches for  
1092 conservation biology: Advantages, limitations and practical recommendations. *Molecular  
1093 Ecology*, 26(20), 5369–5406.

1094 Fumagalli, M. (2013). Assessing the effect of sequencing depth and sample size in population  
1095 genetics inferences. *PLoS One*, 8(11), e79667.

1096 Fumagalli, M., Vieira, F. G., Korneliussen, T. S., Linderroth, T., Huerta-Sánchez, E., Albrechtsen,  
1097 A., & Nielsen, R. (2013). Quantifying population genetic differentiation from next-generation  
1098 sequencing data. *Genetics*, 195(3), 979–992.

1099 Fumagalli, M., Vieira, F. G., Linderroth, T., & Nielsen, R. (2014). ngsTools: methods for  
1100 population genetics analyses from next-generation sequencing data. *Bioinformatics*,  
1101 30(10), 1486–1487.

1102 Futschik, A., & Schlötterer, C. (2010). The Next Generation of Molecular Markers From  
1103 Massively Parallel Sequencing of Pooled DNA Samples. *Genetics*, 186(1), 207–218.

1104 Gaio, D., To, J., Liu, M., Monahan, L., Anantanawat, K., & Darling, A. E. (2019). Hackflex: low  
1105 cost Illumina sequencing library construction for high sample counts (p. 779215). doi:  
1106 10.1101/779215

1107 Galinsky, K. J., Bhatia, G., Loh, P.-R., Georgiev, S., Mukherjee, S., Patterson, N. J., & Price, A.  
1108 L. (2016). Fast Principal-Component Analysis Reveals Convergent Evolution of ADH1B in  
1109 Europe and East Asia. *American Journal of Human Genetics*, 98(3), 456–472.

1110 Garrison, E., & Marth, G. (2012). Haplotype-based variant detection from short-read  
1111 sequencing. arXiv. Retrieved from <http://arxiv.org/abs/1207.3907>

1112 Gatter, T., von Löhneysen, S., Drozdova, P., Hartmann, T., & Stadler, P. F. (2020). Economic  
1113 Genome Assembly from Low Coverage Illumina and Nanopore Data (p.  
1114 2020.02.07.939454). doi: 10.1101/2020.02.07.939454

1115 Gautier, M. (2015). Genome-Wide Scan for Adaptive Divergence and Association with  
1116 Population-Specific Covariates. *Genetics*, 201(4), 1555–1579.

1117 Gignoux-Wolfsohn, S. A., Pinsky, M. L., Kerwin, K., Herzog, C., Hall, M., Bennett, A. B., ...  
1118 Maslo, B. (2021). Genomic signatures of selection in bats surviving white-nose syndrome.  
1119 *Molecular Ecology*. Retrieved from  
1120 <https://onlinelibrary.wiley.com/doi/abs/10.1111/mec.15813>

1121 Gutenkunst, R. N., Hernandez, R. D., Williamson, S. H., & Bustamante, C. D. (2009). Inferring  
1122 the joint demographic history of multiple populations from multidimensional SNP frequency  
1123 data. *PLoS Genetics*, 5(10), e1000695.

1124 Haller, B. C., & Messer, P. W. (2019). SLiM 3: Forward Genetic Simulations Beyond the Wright–  
1125 Fisher Model. *Molecular Biology and Evolution*, 36(3), 632–637.

1126 Han, E., Sinsheimer, J. S., & Novembre, J. (2015). Fast and accurate site frequency spectrum  
1127 estimation from low coverage sequence data. *Bioinformatics*, 31(5), 720–727.

1128 Hayes, B. J., Visscher, P. M., McPartlan, H. C., & Goddard, M. E. (2003). Novel multilocus  
1129 measure of linkage disequilibrium to estimate past effective population size. *Genome*  
1130 *Research*, 13(4), 635–643.

1131 Hennig, B. P., Velten, L., Racke, I., Tu, C. S., Thoms, M., Rybin, V., ... Steinmetz, L. M. (2018).  
1132 Large-Scale Low-Cost NGS Library Preparation Using a Robust Tn5 Purification and  
1133 Tagmentation Protocol. *G3*, 8(1), 79–89.

1134 Huang, W., Li, L., Myers, J. R., & Marth, G. T. (2012). ART: a next-generation sequencing read  
1135 simulator. *Bioinformatics*, 28(4), 593–594.

1136 Jones, F. C., Grabherr, M. G., Chan, Y. F., Russell, P., Mauceli, E., Johnson, J., ... Kingsley, D.  
1137 M. (2012). The genomic basis of adaptive evolution in threespine sticklebacks. *Nature*,  
1138 484(7392), 55–61.

1139 Jørsboe, E., & Albrechtsen, A. (2019). A Genotype Likelihood Framework for GWAS with Low  
1140 Depth Sequencing Data from Admixed Individuals. *bioRxiv*. Retrieved from  
1141 <https://www.biorxiv.org/content/10.1101/786384v1.full-text>

1142 Kim, S. Y., Lohmueller, K. E., Albrechtsen, A., Li, Y., Korneliussen, T., Tian, G., ... Nielsen, R.  
1143 (2011). Estimation of allele frequency and association mapping using next-generation  
1144 sequencing data. *BMC Bioinformatics*, 12, 231.

1145 Korneliussen, T. S., Albrechtsen, A., & Nielsen, R. (2014). ANGSD: Analysis of Next Generation  
1146 Sequencing Data. *BMC Bioinformatics*, 15, 356.

1147 Korneliussen, T. S., & Moltke, I. (2015). NgsRelate: a software tool for estimating pairwise  
1148 relatedness from next-generation sequencing data. *Bioinformatics*, 31(24), 4009–4011.

1149 Kousathanas, A., Leuenberger, C., Link, V., Sell, C., Burger, J., & Wegmann, D. (2017).  
1150 Inferring Heterozygosity from Ancient and Low Coverage Genomes. *Genetics*, 205(1), 317–  
1151 332.

1152 Leitwein, M., Duranton, M., Rougemont, Q., Gagnaire, P.-A., & Bernatchez, L. (2020). Using

1153 Haplotype Information for Conservation Genomics. *Trends in Ecology & Evolution*, 35(3),  
1154 245–258.

1155 Li, H. (2011). A statistical framework for SNP calling, mutation discovery, association mapping  
1156 and population genetical parameter estimation from sequencing data. *Bioinformatics* ,  
1157 27(21), 2987–2993.

1158 Li, H., & Durbin, R. (2011). Inference of human population history from individual whole-genome  
1159 sequences. *Nature*, 475(7357), 493–496.

1160 Li, H., Handsaker, B., Wysoker, A., Fennell, T., Ruan, J., Homer, N., ... 1000 Genome Project  
1161 Data Processing Subgroup. (2009). The Sequence Alignment/Map format and SAMtools.  
1162 *Bioinformatics* , 25(16), 2078–2079.

1163 Li, H., Wu, K., Ruan, C., Pan, J., Wang, Y., & Long, H. (2019). Cost-reduction strategies in  
1164 massive genomics experiments. *Marine Life Science & Technology*, 1(1), 15–21.

1165 Link, V., Kousathanas, A., Veeramah, K., Sell, C., Scheu, A., & Wegmann, D. (2017). ATLAS:  
1166 Analysis Tools for Low-depth and Ancient Samples (p. 105346). doi: 10.1101/105346

1167 Liu, S., Lorenzen, E. D., Fumagalli, M., Li, B., Harris, K., Xiong, Z., ... Wang, J. (2014).  
1168 Population genomics reveal recent speciation and rapid evolutionary adaptation in polar  
1169 bears. *Cell*, 157(4), 785–794.

1170 Li, Y., Sidore, C., Kang, H. M., Boehnke, M., & Abecasis, G. R. (2011). Low-coverage  
1171 sequencing: implications for design of complex trait association studies. *Genome*  
1172 *Research*, 21(6), 940–951.

1173 Lou, R. N., Fletcher, N. K., Wilder, A. P., Conover, D. O., Therkildsen, N. O., & Searle, J. B.  
1174 (2018). Full mitochondrial genome sequences reveal new insights about post-glacial  
1175 expansion and regional phylogeographic structure in the Atlantic silverside (*Menidia*  
1176 *menidia*). *Marine Biology*, 165(8), 124.

1177 Lowry, D. B., Hoban, S., Kelley, J. L., Lotterhos, K. E., Reed, L. K., Antolin, M. F., & Storfer, A.  
1178 (2017). Breaking RAD: An evaluation of the utility of restriction site-associated DNA  
1179 sequencing for genome scans of adaptation. *Molecular Ecology Resources*, 17(2), 142–  
1180 152.

1181 Margaryan, A., Lawson, D. J., Sikora, M., Racimo, F., Rasmussen, S., Moltke, I., ... Willerslev,  
1182 E. (2020). Population genomics of the Viking world. *Nature*, 585(7825), 390–396.

1183 McCartney-Melstad, E., Mount, G. G., & Shaffer, H. B. (2016). Exon capture optimization in  
1184 amphibians with large genomes. *Molecular Ecology Resources*, 16(5), 1084–1094.

1185 McKenna, A., Hanna, M., Banks, E., Sivachenko, A., Cibulskis, K., Kernytsky, A., ... DePristo,  
1186 M. A. (2010). The Genome Analysis Toolkit: a MapReduce framework for analyzing next-  
1187 generation DNA sequencing data. *Genome Research*, 20(9), 1297–1303.

1188 McKinney, G. J., Larson, W. A., Seeb, L. W., & Seeb, J. E. (2017). RADseq provides  
1189 unprecedented insights into molecular ecology and evolutionary genetics: comment on  
1190 Breaking RAD by Lowry et al . (2016). *Molecular Ecology Resources*, 17(3), 356–361.

1191 Medina, P., Thornlow, B., Nielsen, R., & Corbett-Detig, R. (2018). Estimating the Timing of  
1192 Multiple Admixture Pulses During Local Ancestry Inference. *Genetics*, 210(3), 1089–1107.

1193 Meek, M. H., & Larson, W. A. (2019). The future is now: Amplicon sequencing and sequence  
1194 capture usher in the conservation genomics era. *Molecular Ecology Resources*, 19(4), 795–  
1195 803.

1196 Meier, J. I., Salazar, P. A., Kučka, M., Davies, R. W., & Dréau, A. (2020). Haplotype tagging  
1197 reveals parallel formation of hybrid races in two butterfly species. *bioRxiv*. Retrieved from  
1198 <https://www.biorxiv.org/content/10.1101/2020.05.25.113688v1.abstract>

1199 Meisner, J., & Albrechtsen, A. (2018). Inferring Population Structure and Admixture Proportions  
1200 in Low-Depth NGS Data. *Genetics*, 210(2), 719–731.

1201 Meisner, J., Albrechtsen, A., & Hanghøj, K. (2021). Detecting Selection in Low-Coverage High-  
1202 Throughput Sequencing Data using Principal Component Analysis (p. 2021.03.01.432540).  
1203 doi: 10.1101/2021.03.01.432540

1204 Mérot, C., Berdan E., Cayuela H., Djambazian H., Ferchaud A-L., Laporte M., Normandeau E.,  
1205 Ragoussis J., Wellenreuther M., & Bernatchez L. (2021). Locally-adaptive inversions  
1206 modulate genetic variation at different geographic scales in a seaweed fly. *bioRxiv* .  
1207 <https://doi.org/10.1101/2020.12.28.424584>

1208 Nevado, B., Ramos-Onsins, S. E., & Perez-Enciso, M. (2014). Resequencing studies of  
1209 nonmodel organisms using closely related reference genomes: optimal experimental  
1210 designs and bioinformatics approaches for population genomics. *Molecular Ecology*, *23*(7),  
1211 1764–1779.

1212 Nielsen, R., Korneliussen, T., Albrechtsen, A., Li, Y., & Wang, J. (2012). SNP calling, genotype  
1213 calling, and sample allele frequency estimation from New-Generation Sequencing data.  
1214 *PloS One*, *7*(7), e37558.

1215 Nielsen, R., Paul, J. S., Albrechtsen, A., & Song, Y. S. (2011). Genotype and SNP calling from  
1216 next-generation sequencing data. *Nature Reviews. Genetics*, *12*(6), 443–451.

1217 Pasaniuc, B., Rohland, N., McLaren, P. J., Garimella, K., Zaitlen, N., Li, H., ... Price, A. L.  
1218 (2012). Extremely low-coverage sequencing and imputation increases power for genome-  
1219 wide association studies. *Nature Genetics*, *44*(6), 631–635.

1220 Petkova, D., Novembre, J., & Stephens, M. (2016). Visualizing spatial population structure with  
1221 estimated effective migration surfaces. *Nature Genetics*, *48*(1), 94–100.

1222 Picelli, S., Björklund, A. K., Reinius, B., Sagasser, S., Winberg, G., & Sandberg, R. (2014). Tn5  
1223 transposase and tagmentation procedures for massively scaled sequencing projects.  
1224 *Genome Research*, *24*(12), 2033–2040.

1225 Pickrell, J. K., & Pritchard, J. K. (2012). Inference of population splits and mixtures from  
1226 genome-wide allele frequency data. *PLoS Genetics*, *8*(11), e1002967.

1227 Powell, D. L., García-Olazábal, M., Keegan, M., Reilly, P., Du, K., Díaz-Loyo, A. P., ...  
1228 Schumer, M. (2020). Natural hybridization reveals incompatible alleles that cause  
1229 melanoma in swordtail fish. *Science*, *368*(6492), 731–736.

1230 Pritchard, J. K., Stephens, M., & Donnelly, P. (2000). Inference of population structure using  
1231 multilocus genotype data. *Genetics*, *155*(2), 945–959.

1232 Puritz, J. B., & Lotterhos, K. E. (2018). Expressed exome capture sequencing: A method for  
1233 cost-effective exome sequencing for all organisms. *Molecular Ecology Resources*, *18*(6),  
1234 1209–1222.

1235 Rastas, P. (2017). Lep-MAP3: robust linkage mapping even for low-coverage whole genome  
1236 sequencing data. *Bioinformatics* , *33*(23), 3726–3732.

1237 Reed, R. D., Papa, R., Martin, A., Hines, H. M., Counterman, B. A., Pardo-Diaz, C., ... McMillan,  
1238 W. O. (2011). optix drives the repeated convergent evolution of butterfly wing pattern  
1239 mimicry. *Science*, *333*(6046), 1137–1141.

1240 Rice, E. S., & Green, R. E. (2019). New Approaches for Genome Assembly and Scaffolding.  
1241 *Annual Review of Animal Biosciences*, *7*, 17–40.

1242 Ros-Freixedes, R., Whalen, A., Gorjanc, G., Mileham, A. J., & Hickey, J. M. (2020). Evaluation  
1243 of sequencing strategies for whole-genome imputation with hybrid peeling. *Genetics*,  
1244 *Selection, Evolution: GSE*, *52*(1), 18.

1245 Rowan, B. A., Heavens, D., Feuerborn, T. R., Tock, A. J., Henderson, I. R., & Weigel, D. (2019).  
1246 An Ultra High-Density Arabidopsis thaliana Crossover Map That Refines the Influences of  
1247 Structural Variation and Epigenetic Features. *Genetics*, *213*(3), 771–787.

1248 Schlötterer, C., Tobler, R., Kofler, R., & Nolte, V. (2014). Sequencing pools of individuals—  
1249 mining genome-wide polymorphism data without big funding. *Nature Reviews. Genetics*,  
1250 *15*(11), 749–763.

1251 Schumer, M., Powell, D. L., & Corbett-Detig, R. (2020). Versatile simulations of admixture and  
1252 accurate local ancestry inference with mixnmatch and ancestryinfer. *Molecular Ecology*  
1253 *Resources*, *20*(4), 1141–1151.

1254 Shi, S., Yuan, N., Yang, M., Du, Z., Wang, J., Sheng, X., ... Xiao, J. (2018). Comprehensive

1255 Assessment of Genotype Imputation Performance. *Human Heredity*, 83(3), 107–116.  
1256 Skotte, L., Korneliusen, T. S., & Albrechtsen, A. (2012). Association testing for next-generation  
1257 sequencing data using score statistics. *Genetic Epidemiology*, 36(5), 430–437.  
1258 Skotte, L., Korneliusen, T. S., & Albrechtsen, A. (2013). Estimating individual admixture  
1259 proportions from next generation sequencing data. *Genetics*, 195(3), 693–702.  
1260 Slatkin, M. (2008). Linkage disequilibrium--understanding the evolutionary past and mapping the  
1261 medical future. *Nature Reviews. Genetics*, 9(6), 477–485.  
1262 Snyder-Mackler, N., Majoros, W. H., Yuan, M. L., Shaver, A. O., Gordon, J. B., Kopp, G. H., ...  
1263 Tung, J. (2016). Efficient Genome-Wide Sequencing and Low-Coverage Pedigree Analysis  
1264 from Noninvasively Collected Samples. *Genetics*, 203(2), 699–714.  
1265 Szarmach, S., Brelsford, A., Witt, C. C., & Toews, D. (2021). Comparing divergence landscapes  
1266 from reduced-representation and whole-genome re-sequencing in the yellow-rumped  
1267 warbler (*Setophaga coronata*) species .... *bioRxiv*. Retrieved from  
1268 <https://www.biorxiv.org/content/10.1101/2021.03.23.436663v1.abstract>  
1269 Tang, H., Peng, J., Wang, P., & Risch, N. J. (2005). Estimation of individual admixture:  
1270 analytical and study design considerations. *Genetic Epidemiology*, 28(4), 289–301.  
1271 Therkildsen, N. O., & Palumbi, S. R. (2017). Practical low-coverage genomewide sequencing of  
1272 hundreds of individually barcoded samples for population and evolutionary genomics in  
1273 nonmodel species. *Molecular Ecology Resources*, 17(2), 194–208.  
1274 Therkildsen, N. O., Wilder, A. P., Conover, D. O., Munch, S. B., Baumann, H., & Palumbi, S. R.  
1275 (2019). Contrasting genomic shifts underlie parallel phenotypic evolution in response to  
1276 fishing. *Science*, 365, 487–490.  
1277 Tiffin, P., & Ross-Ibarra, J. (2014). Advances and limits of using population genetics to  
1278 understand local adaptation. *Trends in Ecology & Evolution*, 29(12), 673–680.  
1279 Turner, T. L., Hahn, M. W., & Nuzhdin, S. V. (2005). Genomic islands of speciation in  
1280 *Anopheles gambiae*. *PLoS Biology*, 3(9), e285.  
1281 Van Belleghem, S. M., Rastas, P., Papanicolaou, A., Martin, S. H., Arias, C. F., Supple, M.  
1282 A., ... Papa, R. (2017). Complex modular architecture around a simple toolkit of wing  
1283 pattern genes. *Nature Ecology & Evolution*, 1(3), 52.  
1284 VanRaden, P. M., Sun, C., & O'Connell, J. R. (2015). Fast imputation using medium or low-  
1285 coverage sequence data. *BMC Genetics*, 16, 82.  
1286 Vieira, F. G., Albrechtsen, A., & Nielsen, R. (2016). Estimating IBD tracts from low coverage  
1287 NGS data. *Bioinformatics*, 32(14), 2096–2102.  
1288 Vieira, F. G., Fumagalli, M., Albrechtsen, A., & Nielsen, R. (2013). Estimating inbreeding  
1289 coefficients from NGS data: Impact on genotype calling and allele frequency estimation.  
1290 *Genome Research*, 23(11), 1852–1861.  
1291 Vonesch, S. C., Li, S., Tu, C. S., Hennig, B. P., Dobrev, N., & Steinmetz, L. M. (2020). Fast and  
1292 inexpensive whole genome sequencing library preparation from intact yeast cells (p.  
1293 2020.09.03.280990). doi: 10.1101/2020.09.03.280990  
1294 Waples, R. S., & Do, C. (2010). Linkage disequilibrium estimates of contemporary N e using  
1295 highly variable genetic markers: a largely untapped resource for applied conservation and  
1296 evolution. *Evolutionary Applications*, 3(3), 244–262.  
1297 Warmuth, V. M., & Ellegren, H. (2019). Genotype-free estimation of allele frequencies reduces  
1298 bias and improves demographic inference from RADSeq data. *Molecular Ecology*  
1299 *Resources*, 19(3), 586–596.  
1300 Wetterstrand, K. A. (2021). DNA sequencing costs: data from the NHGRI genome sequencing  
1301 program (GSP) [www.genome.gov/sequencingcostsdata](http://www.genome.gov/sequencingcostsdata).  
1302 Whalen, A., Gorjanc, G., & Hickey, J. M. (2019). Parentage assignment with genotyping-by-  
1303 sequencing data. *Journal of Animal Breeding and Genetics = Zeitschrift Fur Tierzuchtug*  
1304 *Und Zuchtungsbiologie*, 136(2), 102–112.  
1305 Whalen, A., Ros-Freixedes, R., Wilson, D. L., Gorjanc, G., & Hickey, J. M. (2018). Hybrid

1306 peeling for fast and accurate calling, phasing, and imputation with sequence data of any  
1307 coverage in pedigrees. *Genetics, Selection, Evolution: GSE*, 50(1), 67.

1308 Whitlock, M. C., & Lotterhos, K. E. (2015). Reliable Detection of Loci Responsible for Local  
1309 Adaptation: Inference of a Null Model through Trimming the Distribution of FST. *The*  
1310 *American Naturalist*, 186(S1), S24–S36.

1311 Wilder, A. P., Palumbi, S. R., Conover, D. O., & Therkildsen, N. O. (2020). Footprints of local  
1312 adaptation span hundreds of linked genes in the Atlantic silverside genome. *Evolution*  
1313 *Letters*, n/a(n/a). doi: 10.1002/evl3.189

1314 Zhu, Y., Bergland, A. O., González, J., & Petrov, D. A. (2012). Empirical validation of pooled  
1315 whole genome population re-sequencing in *Drosophila melanogaster*. *PloS One*, 7(7),  
1316 e41901.

1317 **Table 1. Total cost per sample for both library preparation and sequencing based on**  
 1318 **November 2020 price levels (rounded up to nearest dollar)**  
 1319

Genome size (Gb)	Cost per sample (USD)*		Example organisms
	1x coverage	2x coverage	
0.2	11(3)	13(5)	Fruit fly, Honeybee, Arabidopsis
0.65	16(8)	24(16)	Atlantic silverside, Stickleback, Eastern oyster
1	20(12)	32(24)	Zebra finch, Chicken, Purple sea urchin
3	44(36)	79(71)	Human, Atlantic salmon, African clawed frog

1320  
 1321 \*Cost estimates do not include labor and assume that samples are sequenced efficiently on a HiSeq X  
 1322 Ten system. The assumed costs break down to 8 USD per library (Therkildsen & Palumbi, 2017) and  
 1323 1,300 USD per lane generating 110 Gb sequence data (see supplementary methods for estimates of  
 1324 initial investment costs). The numbers in brackets show the cost of sequencing only (i.e. the approximate  
 1325 total cost with a cheap homebrew library preparation method (see section 2.2)).  
 1326

1327  
1328  
1329

**Table 2. List of published software for the analysis of lcWGS data.** References for each software can be found in the main text (Section 3) or in the supplementary material.

Analysis type		Software						
Analysis	Method	ANGSD	Atlas	MAPGD	vcflib	ngsTools <sup>†</sup>	PCAngsd	Specialised software
<b>SNP identification</b>		✓	✓					BaseVar, EBG, Freebayes, GATK, Reveel, etc.
<b>Population structure</b>	PCA	✓				✓	✓	
	Individual genetic distance	✓	✓			✓		skmer
	Local PCA							lostruct*
	Admixture						✓	Entropy, evalAdmix, ngsAdmix, Ohana
<b>Selection scan</b>	PCA-based; ancestry-corrected						✓	Ohana
<b>Association analysis</b>		✓						SNPTEST
<b>Linkage disequilibrium</b>				✓		✓		GUS-LD, PopLD
<b>Individual relatedness</b>	Relatedness			✓			✓	ngsRelate
	Parentage							AlphaAssign
	Pedigree analysis							WHODAD
<b>Inbreeding</b>	Inbreeding coefficient		✓		✓	✓	✓	ngsRelate
	IBD tracts					✓		
	Runs of homozygosity							bcftools roh
<b>Ancestry relationships</b>	D-statistics/ABBA-BABA	✓	✓		✓			
<b>Linkage map construction</b>								Lep-MAP3
<b>Allele frequency estimation</b>		✓	✓	✓				
<b>Site frequency spectrum</b>		✓				✓		
<b>Within population genetic diversity</b>	$\theta$ estimators (e.g. Watterson's, $\pi$ )	✓	✓			✓		
<b>Within population neutrality stats</b>	e.g. Tajima's D, Fay & Wu's H	✓						
<b>Individual level genetic diversity</b>	Individual heterozygosity	✓	✓	✓				heterozygosity-em
<b>Population differentiation</b>	$F_{ST}$	✓			✓	✓		
	dxy					✓		
<b>Allele frequency differentiation</b>	pFst				✓			
<b>Hardy-Weinberg equilibrium</b>		✓		✓			✓	
<b>Structural variants</b>								svgem
<b>Quality score recalibration</b>		✓	✓					

<b>Ploidy inference</b>								HMMploidy
<b>Genotype imputation</b>								Beagle, LB-Impute, LinkImput, loimpute, NOISYmputer, STITCH, etc.

1330  
1331  
1332  
1333  
1334

† ngsTools is a collection of loosely-connected programs including ngsSim, ngsF, ngsPopGen, ngsUtils, ngsDist, ngs-HMM, and ngsLD

\* lostruct can be used together with custom scripts that perform the PCA e.g. in PCAngsd.

1335  
1336

**Table 3. Key data filters to consider in the analysis of lcWGS data**

Category	Filter	Recommendation
General filters	Base quality	Base quality scores are factored into the calculation of genotype likelihoods, so if they accurately reflect the probability of sequencing error, bases with low scores also carry useful information. However, base quality scores are sometimes miscalibrated, so noise may be reduced if bases with scores below a threshold, e.g. 20, are either trimmed off prior to analysis or ignored.
	Mapping quality	Mapping quality is not considered in genotype likelihood estimation in currently available tools, so it is often advisable to remove low-confidence and/or non-uniquely mapped reads prior to analysis. Filtering out reads that do not map in proper pairs should also further increase confidence in reads being mapped to the correct location, but could cause biases in regions with structural variation
	Minimum depth and/or number of individuals	To avoid sites with low or confounding data support in downstream analysis, minimum depth and/or minimum individual filters can be used to exclude sites with much reduced sequencing coverage compared to the rest of the dataset (e.g. regions with low mapping rates, such as repetitive sequences). Appropriate thresholds will vary between data sets, but could e.g. be to exclude sites with read data for <50% of individuals (globally or within each population), or with <0.8x average depth across individuals.
	Maximum depth	Maximum depth filters are used to exclude sites with exceptionally high coverage (e.g. regions that are susceptible to dubious mapping, such as copy number variants or paralogs). Common maximum depth thresholds are one or two standard deviations above the median genome-wide depth.
	Duplicate reads	PCR duplicates can give inflated impressions of how many unique molecules have been sequenced, which - particularly in the presence of preferential amplification of one allele - could bias genotype likelihood estimation. We therefore recommend removing duplicate reads prior to any analysis.
	Indels	Reads mapped to indels are frequently misaligned, especially if the ends of reads span an indel. To avoid false SNPs, we recommend either realigning reads covering an indel or excluding bases flanking indels

Filters on polymorphic sites*	p-value	The significance threshold (often in the form of maximum p-value) can be adjusted to fine-tune the sensitivity of polymorphism detection, with lower p-values leading to fewer, but higher-confidence, SNP calls. A commonly used cut-off is $10^{-6}$
	SNPs with more than two alleles	Most software programs for downstream analyses assume that all SNPs are biallelic, so SNPs with more than two alleles can be filtered out in the SNP identification step to avoid violation of such assumptions.
	Minimum minor allele frequency (MAF)	For many types of analysis, e.g. PCA, admixture analysis, detection of $F_{ST}$ outliers and estimation of LD, low-frequency SNPs are uninformative and can even bias results. For those types of analysis, imposing a minimum MAF filter of 1-10% can substantially speed up computation time. Appropriate thresholds depend on coverage, sample size (how many copies does a MAF threshold correspond to) and the type of downstream analysis.
Restrict analysis to a predefined site list	List of global SNPs	For comparison of parameter estimates for multiple populations, it is important to ensure that data are obtained for a shared set of sites and that SNP polarization (which allele we track the frequency of) is consistent. For programs like ANGSD where population-specific estimates are obtained by analyzing the data from each population separately, a good strategy is to first conduct a global SNP calling with all samples and restrict population-specific analysis to those SNPs with consistent major and minor allele designations and no MAF or SNP p-value filter (because that would give “missing data” if a site is fixed in a particular population).

1337  
1338  
1339  
1340  
1341

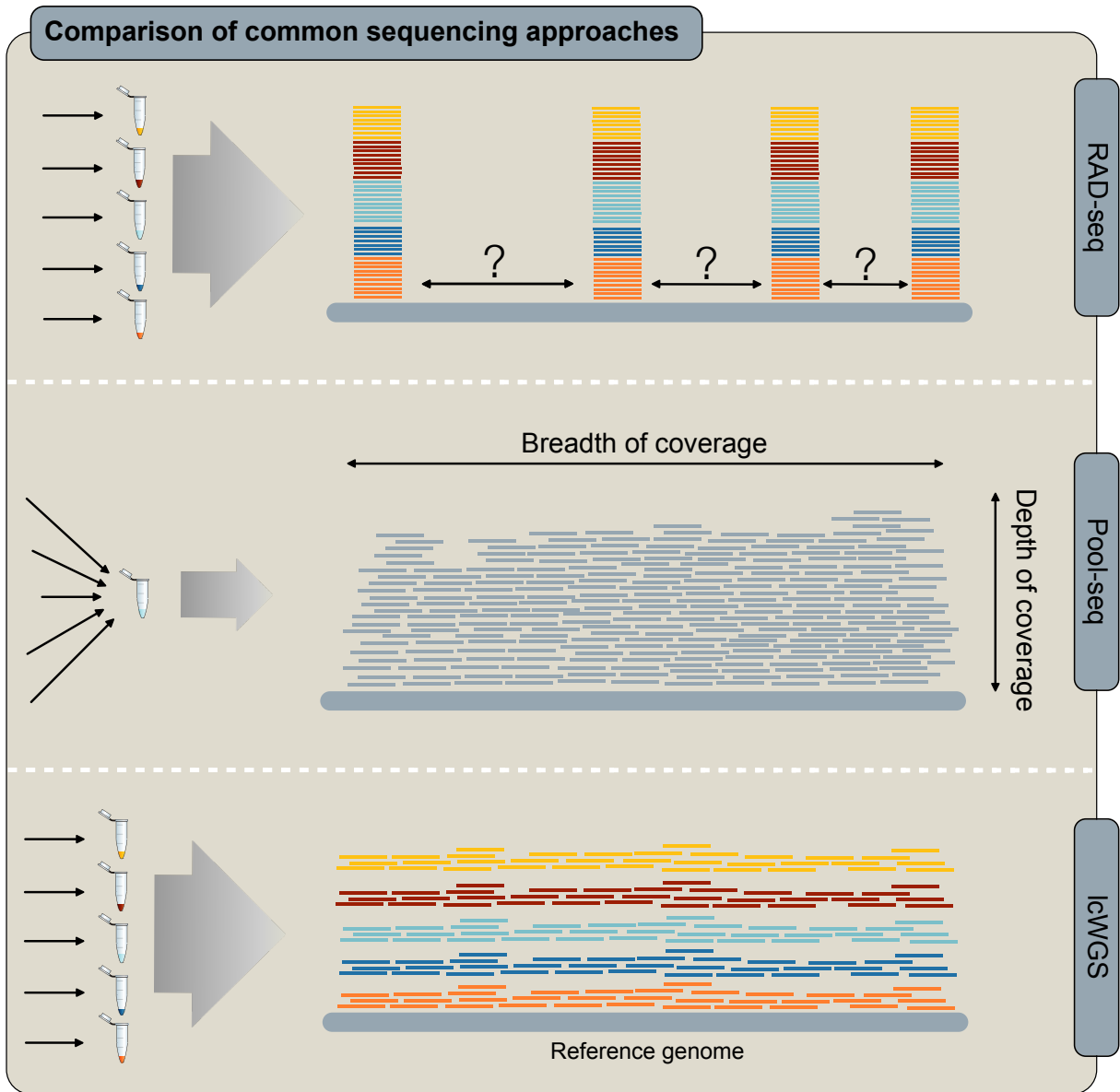
\* Note that no SNP significance or minimum MAF threshold should be used to estimate genetic diversity (e.g. theta and the SFS) as all sites contain relevant information. This also applies to the estimation of the absolute values of  $d_{xy}$ .

1342  
 1343  
 1344  
 1345

**Table 4. Experimental design recommendations for different types of population genomic analyses using lcWGS data**

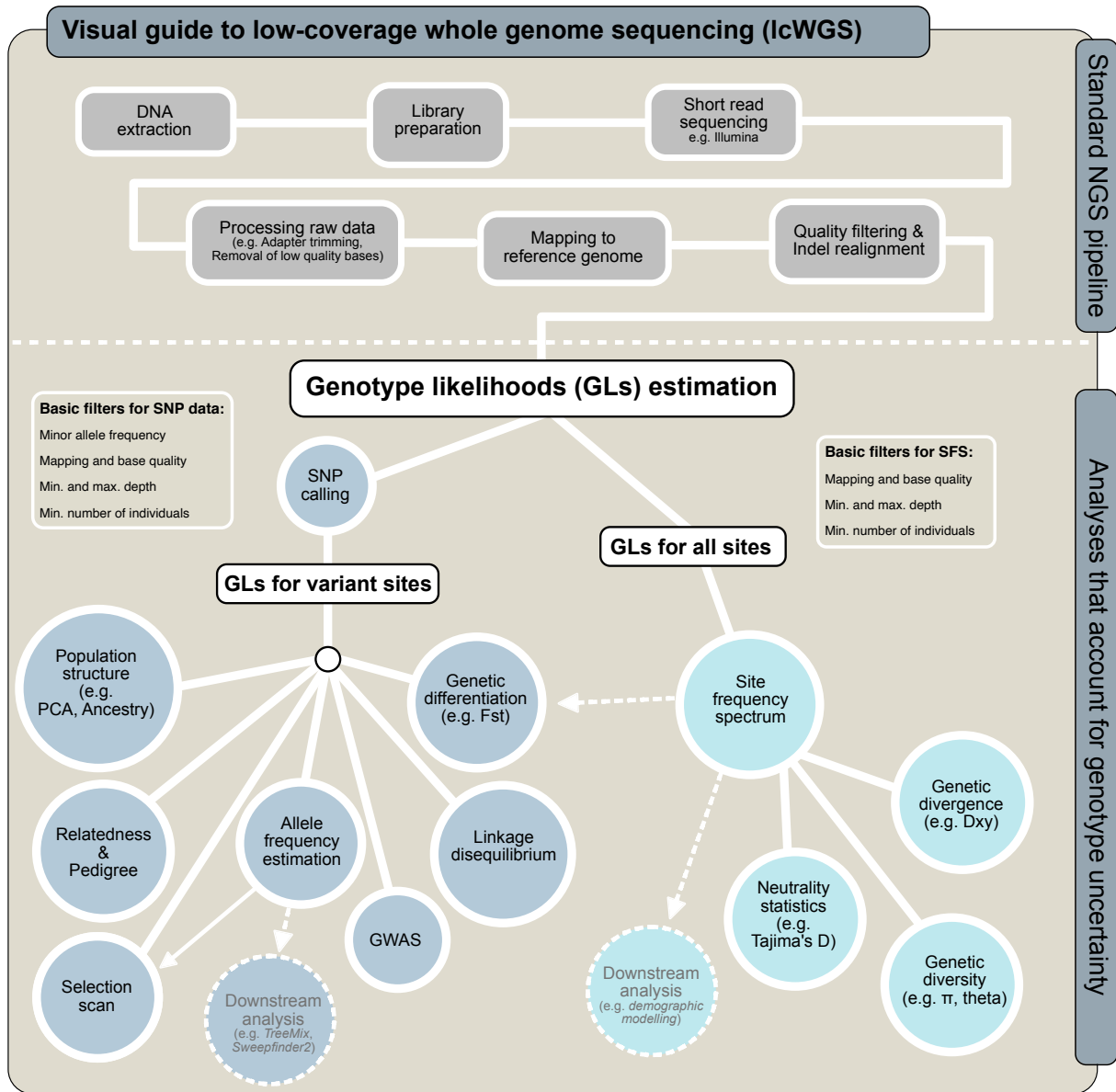
Type of analyses	Examples	Recommendations on experimental design
Allele frequency and differentiation	Allele frequency trajectory, BayPass, $F_{ST}$ (as implemented in vcflib), $\rho F_{st}$	Prioritize larger sample sizes, $\geq 10$ samples per population, $\geq 10x$ coverage per population (Figure 3, 4)
SFS-based analyses (absolute estimation of rare-allele-dependent metrics)	Absolute estimation of Watterson's $\theta$ , Tajima's $D$ , individual heterozygosity $\delta a \delta i$	Prioritize higher coverage per sample, $> 4x$ coverage per sample, $\geq 5$ samples per population (Figure S2, S3)
SFS-based analyses (relative estimation of rare-allele-dependent metrics, or non-rare-allele-dependent metrics)	Relative estimation of Watterson's $\theta$ and Tajima's $D$ (e.g. for outlier scan) $\pi$ , $d_{xy}$ , $F_{ST}$ (as implemented in ANGSD)	Prioritize larger sample sizes, $\geq 10$ samples per population, $\geq 10x$ coverage per population (Figure 6, S2-3, S10-11)
Population structure	PCA, admixture	Prioritize larger sample sizes, $\geq 10$ samples per population, extremely low per-sample coverage (e.g. 0.125x, Figure 5, S9) or highly uneven per-sample coverage (e.g. 0.5-6x, Skotte et al. 2013) could be viable
Absolute estimation of linkage disequilibrium	LD decay rate, demographic inference	Prioritize higher coverage per sample, $\geq 4x$ coverage per sample, $\geq 20$ samples per population (Figure S4, S5; Bilton et al., 2018; Fox et al., 2019; Maruki & Lynch, 2014)
Relative estimation of linkage disequilibrium	LD pruning, LD block identification	Per-sample coverage as low as 1x could be viable, $\geq 20x$ coverage per population (Figure S4, S5)
Genotype imputation without reference panels	STITCH, Beagle	STITCH: prioritize larger sample size ( $\geq 500$ ) over per-sample coverage (1x could be sufficient) Beagle: prioritize higher per-sample coverage ( $\geq 2x$ ) over sample sizes ( $\leq 250$ could be sufficient) (Figure 9)

1346



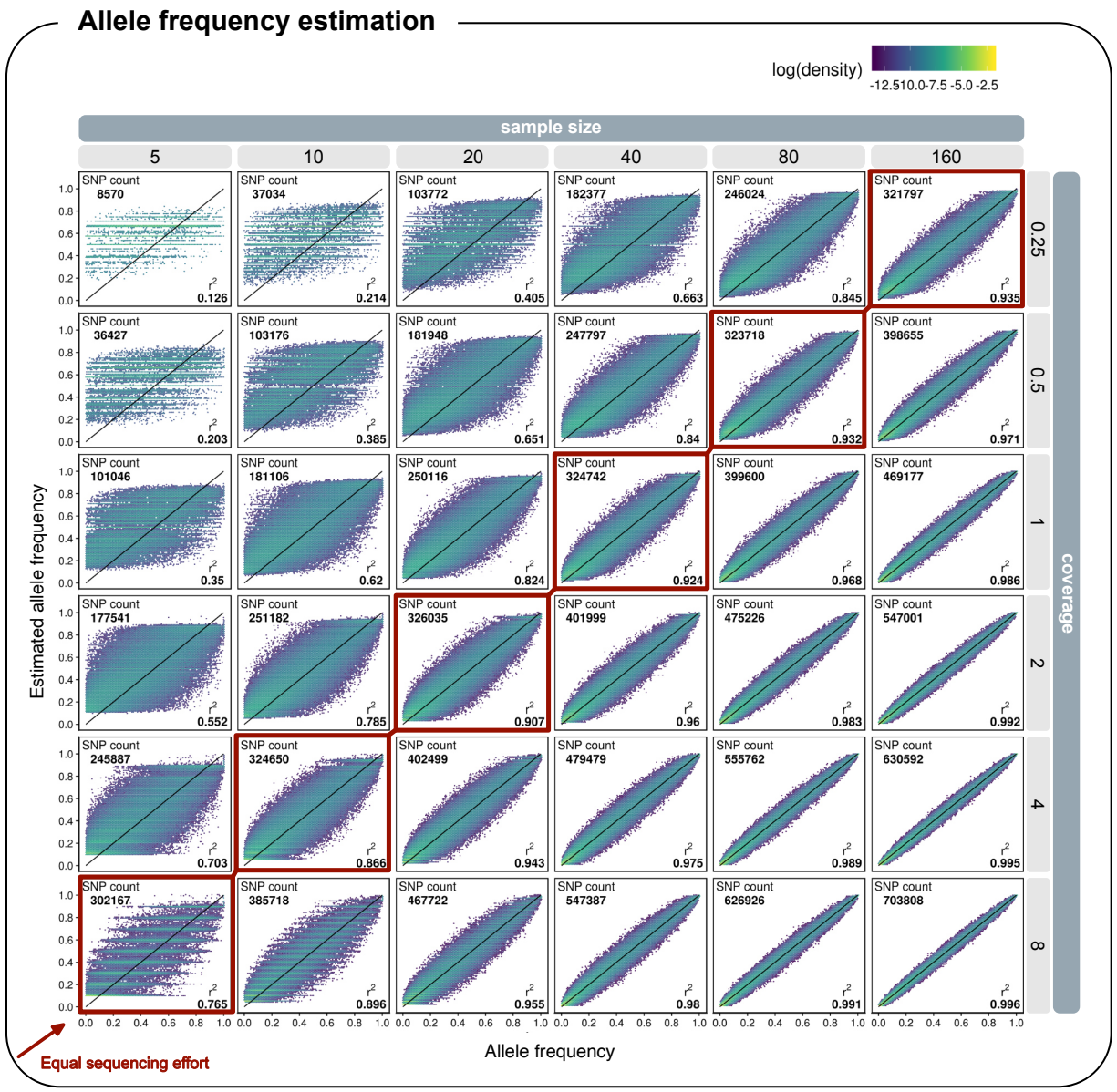
1347  
 1348  
 1349  
 1350

**Figure 1.** Diagram showing the distribution of sequencing reads mapped to a reference genome under (A) a RAD-seq, (B) a Pool-seq, and (C) a lcWGS design.



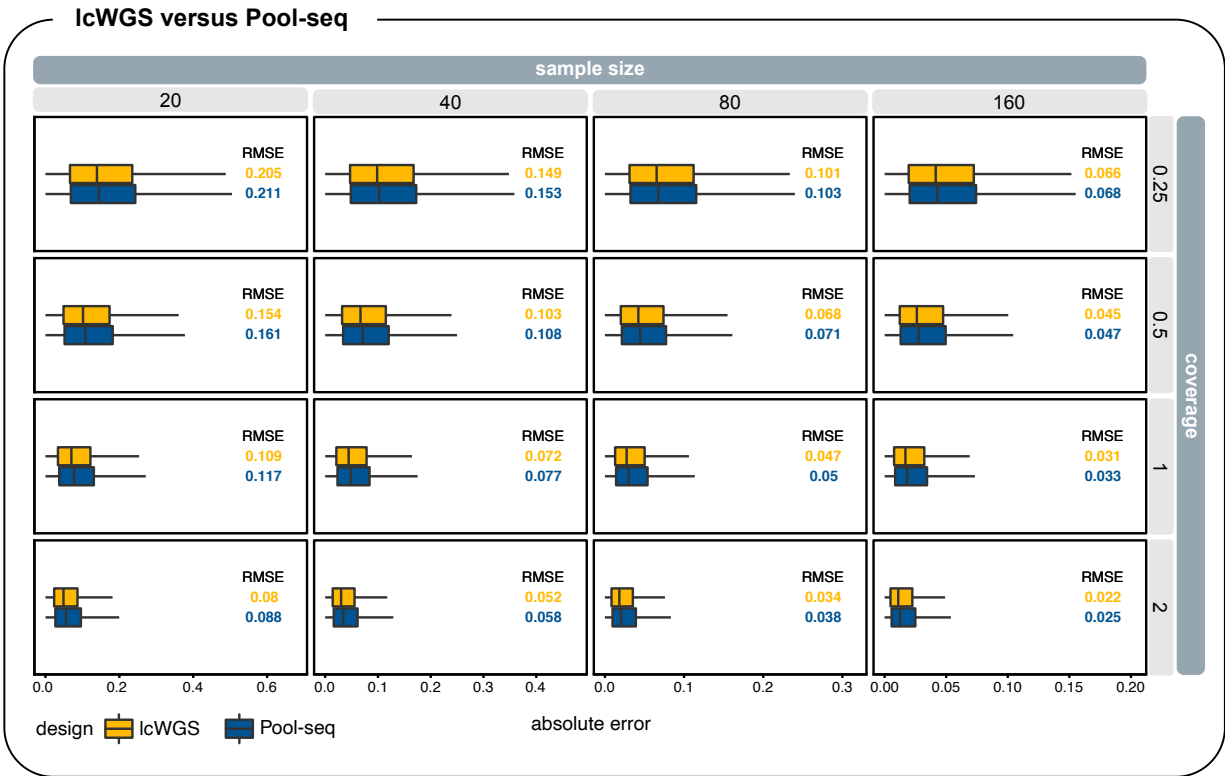
1351  
 1352  
 1353  
 1354  
 1355  
 1356

**Figure 2.** Diagram showing a typical computational pipeline for lcWGS data. **Top:** the data processing part of the pipeline, which is similar to the pipeline for other types of NGS data. **Bottom:** the data analysis part of the pipeline, which is based on a probabilistic framework using genotype likelihood to account for genotype uncertainty.

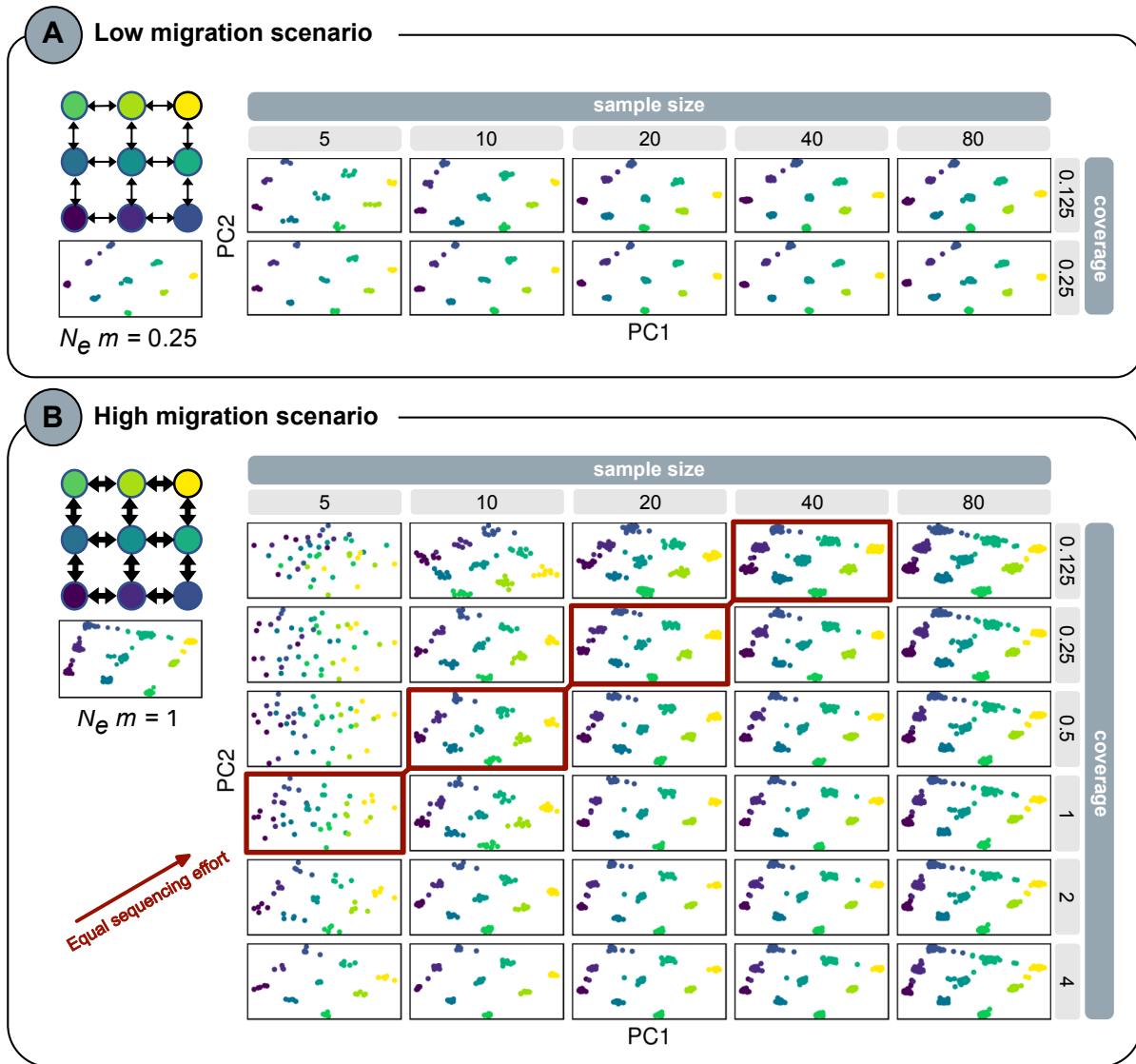


1357  
1358  
1359  
1360  
1361  
1362  
1363  
1364  
1365  
1366  
1367  
1368

**Figure 3.** The estimated vs. true allele frequencies at all called SNPs (i.e. true positives + false positives) with lcWGS. Across the different facets, sample size increases from left to right, and coverage increases from top to bottom. The total sequencing effort remains the same along the diagonal from bottom left to top right. The color indicates the density of points in the area, with yellow corresponding to the highest density and dark blue corresponding to the lowest density.  $r^2$  and the number of SNPs called (SNP count) are shown in each facet. The black line in each facet indicates the positions where the estimated allele frequency is equal to the true allele frequency. False negative SNPs are not included in this figure; their distribution is shown in Figure S1.

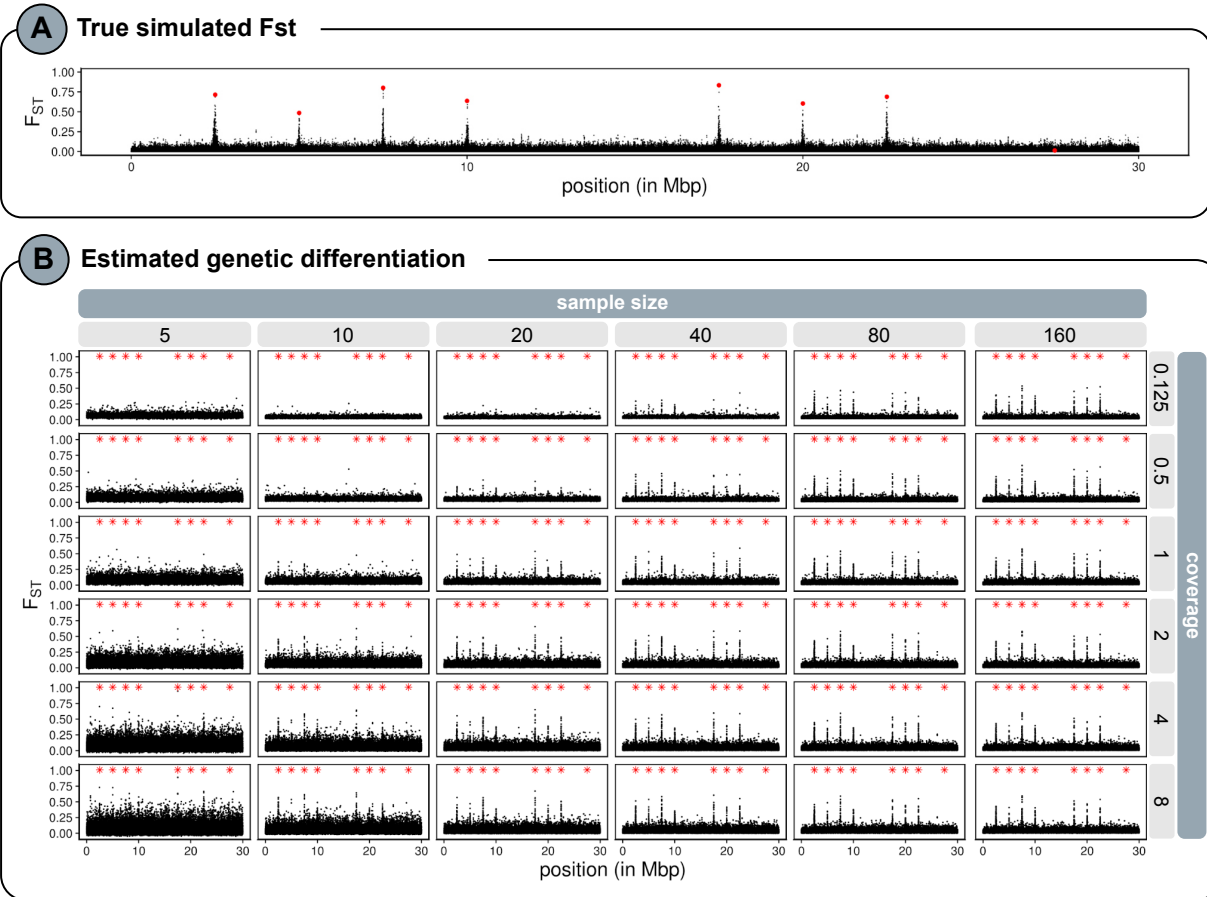


1369  
 1370 **Figure 4.** The error in allele frequency estimation with IcWGS (yellow) and Pool-seq (blue) data.  
 1371 The distribution of absolute errors (|estimated frequency - true frequency|) is shown with the box  
 1372 plots along the x-axis. The lower and upper hinges of the box plots show the interquartile ranges  
 1373 of absolute errors, and the whiskers extend to the largest or smallest values no further than 1.5  
 1374 times the interquartile range. Outlier points are hidden. Across the different facets, sample size  
 1375 increases from left to right, and coverage increases from top to bottom. The total sequencing  
 1376 effort remains the same along the diagonal from bottom left to top right. The root mean squared  
 1377 error (RMSE) for the two sequencing designs are shown in each facet; note the differences in  
 1378 scale of the x-axes. False negative SNPs are not included in this figure; their distribution is  
 1379 shown in Figure S1.  
 1380  
 1381



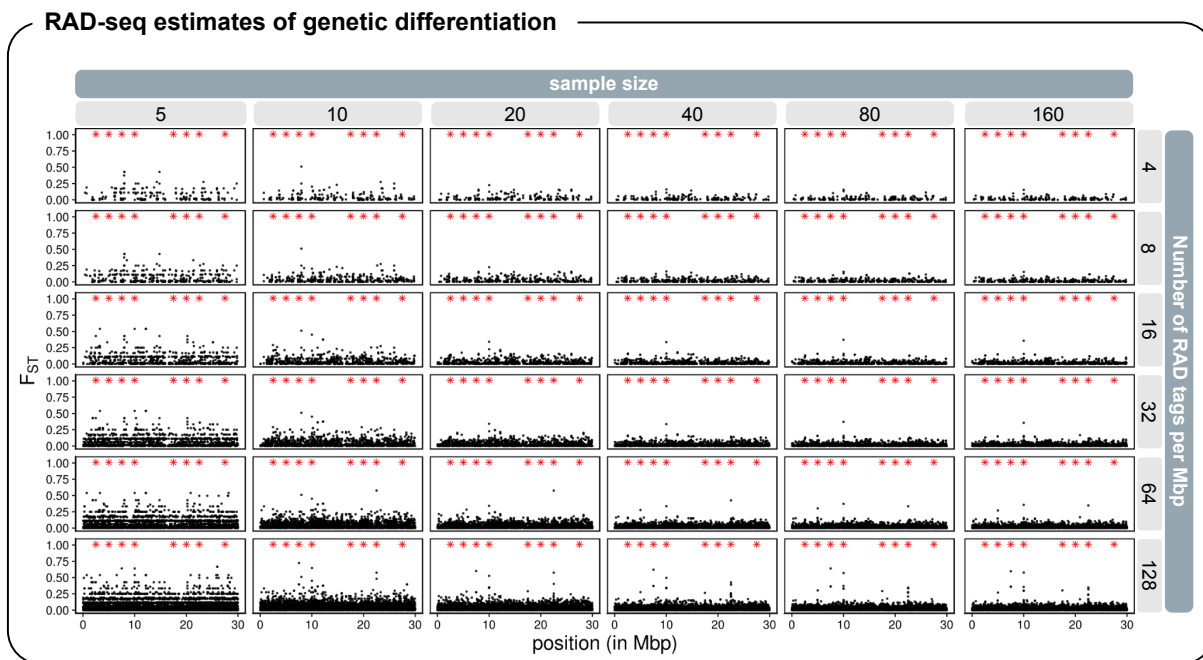
1382  
 1383  
 1384  
 1385  
 1386  
 1387  
 1388  
 1389  
 1390  
 1391  
 1392  
 1393

**Figure 5.** Patterns of spatial population structure inferred through principal component analysis (PCA) with lcWGS data. **(A)** A scenario with lower gene flow (an average of 0.25 effective migrants per generation). **(B)** A scenario with higher gene flow (an average of 1 effective migrant from one population to another every generation). Left: the true population structures being simulated; each node corresponds to a simulated population. Right: the first two principal components from the PCA with simulated lcWGS data; each point corresponds to an individual sample and its color corresponds to the population it is sampled from. Sample size per population increases across panels from left to right, and coverage per sample increases from top to bottom.

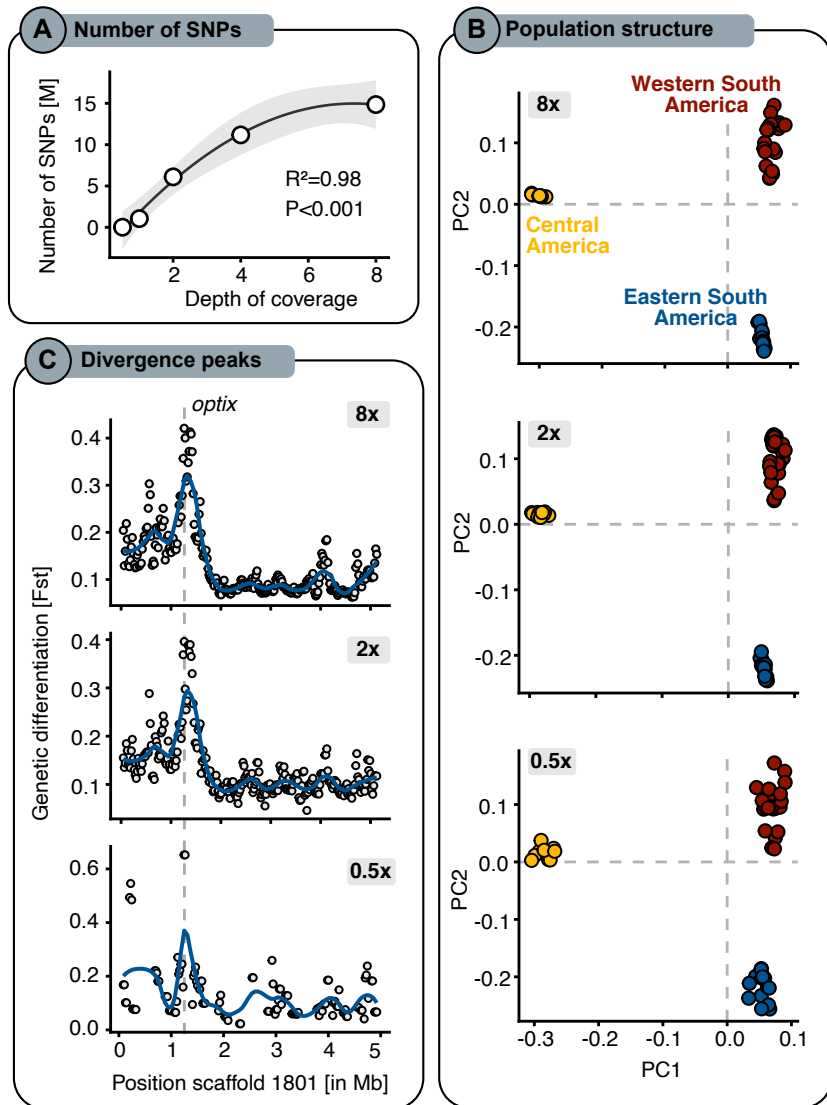


1394  
 1395  
 1396  
 1397  
 1398  
 1399  
 1400  
 1401  
 1402  
 1403

**Figure 6.** Genome-wide scan for divergent selection with lcWGS data. **(A)** The true per-SNP  $F_{ST}$  values along the chromosome between the two simulated populations. **(B)** The  $F_{ST}$  values inferred from lcWGS data in 1kb windows along the chromosome. Sample size per population increases from left to right, and coverage per sample increases from top to bottom. In **(A)**, the red points mark the position of SNPs under selection and the black points mark the neutral SNPs. In **(B)**, the black points mark both the selected and neutral SNPs, and the red asterisks only mark the positions of the selected SNPs (not their inferred  $F_{ST}$  values).

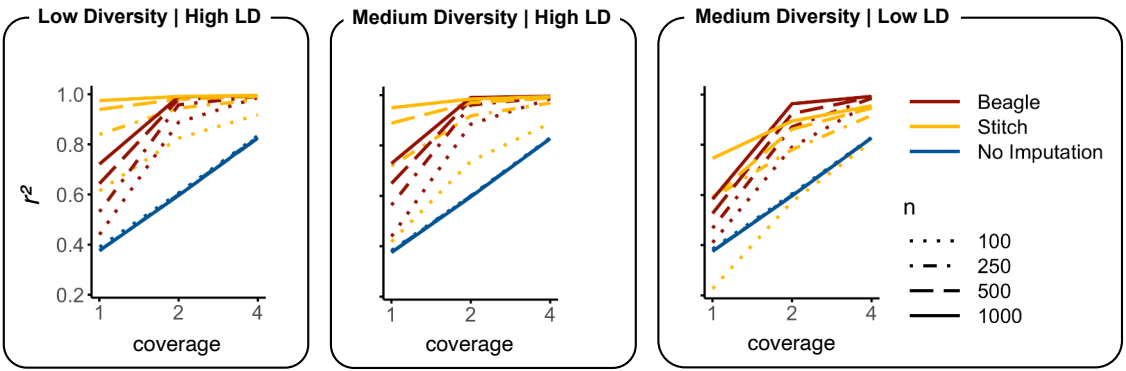


1404  
 1405 **Figure 7.** Genome-wide scan for divergent selection with RADseq data. The per-SNP  $F_{ST}$   
 1406 values inferred from RADseq data are shown on the y axis and the SNP positions are shown on  
 1407 the x axis. Sample size per population increases from left to right, and RAD tag density  
 1408 increases from top to bottom. The black points mark both the selected and neutral SNPs, and  
 1409 the red asterisks only mark the positions of the selected SNPs (not their inferred  $F_{ST}$  values).  
 1410  
 1411



1412  
1413  
1414  
1415  
1416  
1417  
1418  
1419  
1420  
1421  
1422  
1423  
1424  
1425

**Figure 8.** Application of genotype likelihoods to empirical data. **(A)** Correlation between the number of identified SNPs (in millions) with variation in depth of sequencing coverage in the downsampled *Heliconius* dataset. **(B)** Principal components analysis for three different coverages (8x, 2x and 0.5x) of 51 samples. Estimates of population structure are highly concordant across coverages. Subspecies are pooled and colored by their broader region of origin. **(C)** Estimates of genetic differentiation ( $F_{ST}$ ) between pooled *Heliconius* subspecies with the red-bar phenotype ( $n=23$ ) and without the red-bar phenotype ( $n=28$ ) along the scaffold containing the causal *optix* candidate genes in 50kb sliding windows with 20kb steps.  $F_{ST}$  estimates are highly concordant between 8x and 2x coverage, but more sparse at 0.5x due to the lower number of identified variant sites.



1426  
 1427  
 1428  
 1429  
 1430  
 1431  
 1432

**Figure 9.** Genotype imputation in STITCH and Beagle compared to posterior genotypes estimated without imputation in three in populations with varying diversity and linkage disequilibrium.  $r^2$  between true genotypes and estimated genotype dosages are shown for combinations of sample size (n; with increasing n indicated by more contiguous lines), sequencing coverage (x-axis) and method (line colors).